

1     **Analysis of operation performance of three indirect expansion solar assisted air source heat**  
2                                   **pumps for domestic heating**

3  
4     Li Wei Yang<sup>a</sup>, Nan Hua<sup>a</sup>, Jin Huan Pu<sup>a</sup>, Yu Xia<sup>a</sup>, Wen Bin Zhou<sup>b</sup>, Rong Ji Xu<sup>c</sup>, Tong Yang<sup>d</sup>, Yerzhan  
5                                   Belyayev<sup>e</sup>, Hua Sheng Wang<sup>a\*</sup>  
6

7     <sup>a</sup>School of Engineering and Materials Science, Queen Mary University of London, Mile End Road,  
8                                   London E1 4NS, UK

9     <sup>b</sup>Department of Mechanical Engineering, Imperial College London, London SW7 2AZ, UK

10     <sup>c</sup>Beijing University of Civil Engineering and Architecture, Beijing 100044, China

11     <sup>d</sup>Faculty of Science and Technology, Middlesex University, London NW4 4BT, UK

12     <sup>e</sup>Department of Mechanics, Al-Farabi Kazakh National University, Almaty, Al-Farabi ave.71,  
13                                   050040, Kazakhstan  
14

15     **Abstract**

16             To achieve the goal set for net-zero emissions of greenhouse gases in the UK by 2050, the  
17     domestic heating must be decarbonised. Solar assisted air source heat pumps, integrating solar  
18     collector, thermal energy storage tank and heat pump, offers a promising alternative application under  
19     the UK weather conditions. Literature review shows that investigations of solar assisted air source  
20     heat pumps in the regions like the UK are still insufficient. The serial, parallel and dual-source indirect  
21     expansion solar assisted air source heat pumps are modelled and simulated under the weather  
22     conditions in London using TRNSYS to investigate the operation performance over a typical year.  
23     These three heat pumps are applied to provide space heating and hot water of 300 L per day for a  
24     typical single-family house. The simulation results show comparisons of the three systems. The serial  
25     type heat pump shows the highest seasonal performance factor of 5.5, but requiring the largest sizes  
26     of the solar collector and thermal energy storage tank. The dual-source and parallel type heat pumps  
27     show slightly lower seasonal performance factors of 4.4 and 4.5, respectively, requiring smaller sizes  
28     of solar collector and thermal energy storage tank. Furthermore, the results show that the air source  
29     part contributes to an important proportion of the **heat** provision and stable operation of the systems.  
30     The yearly seasonal performance factor higher than 4.4 achievable by the three heat pumps suggests  
31     that they are potentially applied in the regions with relatively lower solar irradiance. The economic  
32     analyses indicate that the parallel and dual-source type heat pumps provide good alternatives to  
33     replacing the gas-boiler heating system.  
34

---

\* Corresponding to: H.S. Wang, School of Engineering and Materials Science, Queen Mary University of London, Mile End Road,  
London E1 4NS, UK  
TEL: +44 (0)20 7882 7921  
E-mail: h.s.wang@qmul.ac.uk

## 35 **Highlights**

36

- 37 • Three indirect expansion solar assisted air source heat pumps are numerically studied.
- 38 • Space heating and hot water performances of three heat pumps are examined in detail.
- 39 • Their yearly seasonal performance factors are higher than 4.4 in high latitude regions.
- 40 • The heat pumps are economically applicable in high latitude regions.

41

42 **Keywords:** Solar assisted air source heat pump, Seasonal performance factor, Domestic heating,  
43 Solar thermal energy, Numerical simulation

44

## 45 **1. Introduction**

46 In the UK, in 2017, space heating (SH) and hot water (HW) took up 80% of the total energy  
47 consumption in the domestic sector [1]. To meet the goal of the net-zero emissions of greenhouse  
48 gases by 2050, the domestic heating must be decarbonised [2]. To compensate the intermittency of  
49 solar energy availability, solar thermal energy [3] can be integrated with heating technologies [4].  
50 Solar-assisted air source heat pump (SAASHP), combining solar thermal energy storage and heat  
51 pump (HP) [5], is promising to achieve the decarbonised domestic heating [6].

52 SAASHPs include direct expansion SAASHPs (DX-SAASHPs) and indirect expansion  
53 SAASHPs (IX-SAASHPs). In the DX-SAASHPs, the solar collector serves as the evaporator. In the  
54 IX-SAASHPs, the solar collector transfers heat to the water which is circulated either through the  
55 evaporator of the heat pump or through the heat exchanger in the thermal energy storage (TES) tank.  
56 IX-SAASHPs have shown high potential for domestic SH and HW [7]. The serial, parallel and dual-  
57 source IX-SAASHPs have been developed.

58 In the past two decades, many investigations of IX-SAASHPs for SH and/or HW in the domestic  
59 heating sector have been conducted. Table 1 summarises some earlier studies on SAASHPs operation  
60 in relatively higher latitude regions. Summaries of more studies on SAASHPs are given in [7].  
61 Freeman et al. [8] numerically simulated three types of IX-SAASHPs for SH of a room with the floor  
62 area 120 m<sup>2</sup> and HW of 279.5 L per day. The averaged *COPs* of these heating systems are 2.0 for  
63 parallel IX-SAASHP, 2.5 for dual-source IX-SAASHP and 2.8 for serial IX-SAASHP. Fraga et al.  
64 [9] monitored the performance of a serial IX-SAASHP providing SH and HW for an apartment block  
65 with a floor area of 927 m<sup>2</sup> (80 flats). The seasonal performance factor (*SPF*) of this IX-SAASHP is  
66 2.9. Ji et al. [10] reported measurements of a triple-functional dual-source IX-SAASHP for SH, space  
67 cooling (SC) and HW using an enthalpy-difference test facility. The *COPs* of the system range from  
68 1.75 to 3.0 in the HW operation mode and from 2.35 to 2.75 in the SH operation mode. Further  
69 experimental studies of this system using a larger water TES tank show the averaged *COP<sub>s</sub>* of 2 - 3.25

70 and 2.25 - 2.5, respectively [11]. Poppi et al. [12] numerically simulated two parallel IX-SAHPs  
71 providing SH and HW for single family houses (SFH) named as 45 and 100. The *SPFs* of the two IX-  
72 SAHPs vary from 2.43 to 3.85 when the ambient temperatures are -10 °C and -5 °C in Zurich and  
73 Carcassonne, respectively. Liu et. al. [13] presented measurements of a dual-source IX-SAASHP for  
74 SH and HW using a novel composite heat exchanger as the evaporator. The *COP* of the system ranges  
75 from 2.0 to 3.1. Ran et al. [14] numerically simulated the performance of a dual-source IX-SAASHP  
76 for SH and HW operation in cities of Lhasa, Chengdu, Beijing and Shenyang in China having  
77 significantly different weather conditions. The *SPFs* of the system operation in these locations are  
78 6.92, 3.61, 3.27 and 2.45, respectively. The latitudes of these locations are below 50°. The high *SPF*  
79 of the system operation in Lhasa plateau is attributed to the high solar irradiance due to the extremely  
80 high elevation.

81 Some studies have been reported for applications of SAASHPs in relatively high latitude regions.  
82 Kutlu et al. [15] numerically simulated a serial IX-SAASHP using phase change material (PCM) for  
83 TES and the evacuated-tube solar collector for HW. The evacuated tube reduces the heat loss and  
84 hence increases the collector efficiency. The *COP* of the system achieves from 3.4 to 4.6 under the  
85 UK summer weather conditions. Yerdesh et al. [16] numerically simulated a solar assisted two-stage  
86 cascade HP for SH and HW under the weather conditions in Kazakhstan. The maximum *COP* of the  
87 system is 2.4 for each stage of the HP using R32 and R290, respectively. Treichel and Cruickshank  
88 [17-19] studied experimentally and numerically a serial IX-SAASHP using a novel air-type solar  
89 collector for HW under the Canadian weather conditions. The *COP* of the system ranges from 1.9 to  
90 2.4. Ma et al. [20] numerically studied the applicability of a two-stage serial IX-SAASHP, using  
91 R410A and CO<sub>2</sub> as the working fluids, for SH under the weather conditions in Canada.

92 This work aims to investigate the feasibility for applications of SAASHPs in relatively high  
93 latitude regions such as London in the UK (51.5° N). A typical single-family house is taken from a  
94 reference building given in the International Energy Agency (IEA) Standard [21] with geometrical  
95 dimensions and relevant properties. The serial, parallel and dual-source type IX-SAASHPs are used  
96 to provide SH and HW of 300 L per day. The three types of IX-SAASHPs are modelled and simulated  
97 using TRNSYS 17 based on a typical meteorological year. The *SPF* and economic performance of  
98 the SAASHPs are compared in view of the electricity generation scenarios and the guidelines to adopt  
99 heat pumps under the net zero carbon emission in the UK by 2050. For the purpose of comparing the  
100 true characteristics of the heating systems, auxiliary heater is not considered in this work.

101

102

Table 1: Summary of some earlier studies on SAASHPs operation in relatively higher latitude regions

Authors	Location	Function	Refrigerant	Collector		Storage volume (m <sup>3</sup> )	$T_{amb}$ (°C)	$HC$ (kW)	$COP$	$SPF$	System category
				Type	Area (m <sup>2</sup> )						
Freeman et al., 1979 [8]	Madison, USA 43°N	SH for a room of 120 m <sup>2</sup> , HW of	-	FPC	10, 20 30, 40 50, 60	0.075 per m <sup>2</sup> solar collector	-	1.95 (SH), 0.68 (SH)	2 (parallel) 2.5 (dual-source)		Parallel IX-SAASHP, Dual-source IX-SAASHP, Serial IX-SAASHP
	Albuquerque, USA 35°N	279.5 L daily						0.94 (SH), 0.68 (SH)	2.8 (serial)		
	Charleston, USA 38°N							0.485 (SH), 0.68 (SH)			
Fraga et al., 2015 [9]	Geneva, Switzerland 46 °N	SH for a block of 927 m <sup>2</sup> , HW	-	bare FPC	116	6 + 0.3×8	-2.4-20.5	2.13 (SH), 5.28 (SH)	-	2.9	Serial IX-SAASHP
Ji et al., 2015 [10]	Hefei, China 32 °N	SH, SC, HW	-	FPC	3.2	0.2	7	1.2-2.4 (HW) 1.4-2.2 (SH)	1.75-3 (HW) 2.35-2.75 (SH)		Dual-source IX-SAASHP
Cai et al., 2016 [11]	Hefei, China 32 °N	SH, SC, HW	-	FPC	3.2	0.3	7	1.9-2.4 (HW) 1.3-1.5 (SH)	2-3.25 (HW) 2.25-2.5 (SH)		
Poppi et al., 2016 [12]	Zurich, Switzerland, 47°N	SH for a room of 140 m <sup>2</sup> , HW	R410A	FPC	9.28	0.763	-10	0.347 (HW), 0.944 (SH)		3.16	Parallel IX-SAASHP
								0.347 (HW),		2.43	

	Carcassonne, France 43°N								1.966 (SH) 0.307 (HW), 0.419 (SH) 0.307 (HW), 1.047 (SH)		3.85	
Liu et al., 2016 [13]	Zhengzhou, China 34°N	SH, HW	-	FPC	-	-	-15, -10, -7, -5, 2, 7	1.2-2.9	2-3.1			Dual-source IX-SAASHP
Ran et al., 2020 [14]	Lhasa, China 29.5°N	SH, HW	-	FPC	300	10	-	120	-	6.92		Dual-source IX-SAASHP
	Chengdu, China 30.7°N							90	-	3.61		
	Beijing, China 40.1 °N							180	-	3.27		
	Shenyang China 41.8°N							270	-	2.45		
Kutlu et al., 2020 [15]	UK	HW	R134a	evacuated tube	4	0.15 (PCM)	9–25	–	3.4–4.6	-		Serial IX- SAASHP
Yerdesh et al., 2020 [16]	Kazakhstan	HW, SH	R134a/R410A, R32/R290, R32/R1234yf, R32/R134a, R410A/R290, R410A/R1234yf, R744/R290, R744/R1234yf, R744/R134a	FPC	6	0.3	-30-10	-	1.8-3	-		A solar assisted cascade HP
Treichel and Cruickshank,	Canada and US	HW	R134a	air-type solar collector	1.26	0.189	-	-	1.9-2.4	-		Serial IX- SAASHP

---

2021 [17], [18], [19] Ma et al., 2020 [20]	Canada	SH	CO <sub>2</sub> , R410A	-	70	3	-6.6- 12.7	-	-	-	A two-stage serial IX- SAASHP
---	--------	----	-------------------------	---	----	---	---------------	---	---	---	-------------------------------------

---

105 **2. Reference building and heat demand**

106 The building of SFH 45 given in the IEA standard [21] is selected as the reference building  
107 for domestic heating. The geometrical dimensions and relevant properties are given in [21].  
108 The indoor floor area of the building is 140 m<sup>2</sup>. The radiant floor is used as the heating method.  
109 Table 2 gives the parameters and their values of TRNSYS module for modelling the  
110 temperature of house ground. Figure 1 shows hourly cooling (positive) and heating (negative)  
111 loads of the house SFH 45 at room air temperature  $T_{room}$  of 18 °C over a typical year of weather  
112 conditions in London. The peak and the averaged heating loads are seen to be 3.15 kW and  
113 1.24 kW, respectively.

114  
115 Table 2: TRNSYS module for modelling the temperature of house ground

116

Component	Module	Parameter	Value
Ground temperature	Type 501	Mean surface Temperature	10.78 °C
		Amplitude of surface temperature	18.04 °C
		Time shift	12 <sup>th</sup> day
		Depth at point	0.445 m

117  
118  
119

120 For the reference building of SFH 45, IEA recommends the SH period to be days when  
121 the 24-hour averaged ambient air temperature is below 14 °C. Under the weather conditions in  
122 London, the results show that the SH period is from 0 to 2736 hour and from 7224 hour to 8760  
123 hour of the year, corresponding to the heating season from 1st October to 30th April. The rest  
124 period of the days is the non-heating season.

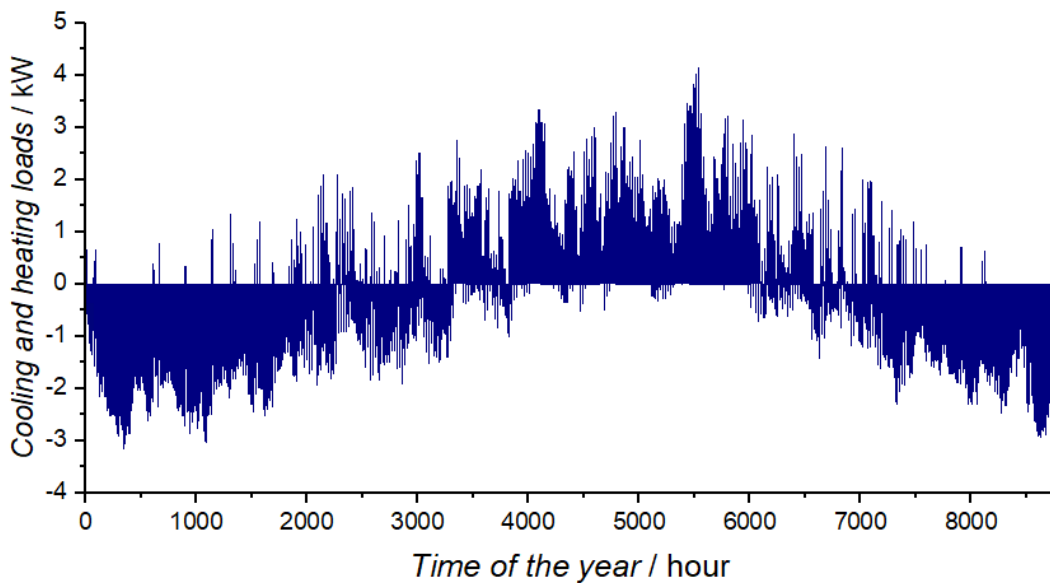


Figure 1: Hourly cooling (positive) and heating (negative) loads of the house SFH 45 at room air temperature  $T_{room}$  of 18 °C over a typical year of weather conditions in London.

### 129 3. Description of the heating systems

130 In this work, serial, parallel and dual-source IX-SAASHPs are modelled and simulated  
131 using TRNSYS 17. Water is used as the medium to transport heat and to store thermal energy.  
132 Refrigerants R134a and R410A are used as the working fluids of SWHP and ASHP,  
133 respectively. In each HP system, two water tanks are employed for TES. One tank stores  
134 thermal energy collected by the solar collector and the other serves as TES for the end use i.e.  
135 providing HW and/or SH. Details about the systems are described below.

136

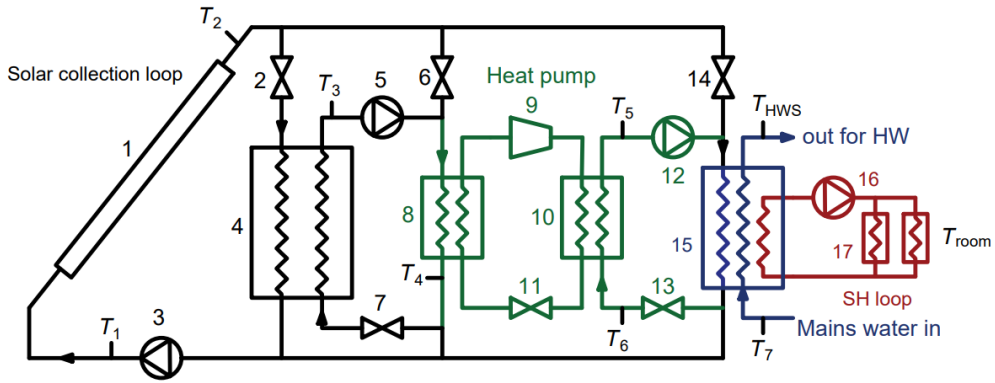
#### 137 3.1 Serial system

138 Figure 2(a) shows a serial IX-SAASHP system, which consists of a solar collection loop  
139 (in black), a SWHP unit (in green), a HW loop (in blue) and a SH loop (in red). The solar  
140 collector converts solar energy into thermal energy and the heat is transferred to water being  
141 circulated by pump 1 (3). The thermal energy is normally stored in the TES tank 1 (valve 2  
142 open) but the hot water can also be circulated to either SWHP (valves 2 and 14 closed, valve 6  
143 open) or to the TES tank 2 (valves 2 and 6 closed, valve 14 open). The SWHP consists of a  
144 water-to-refrigerant evaporator (8), a compressor (9), a condenser (10), and an expansion valve  
145 (11). When the SWHP is in operation, the TES tank 1 (4) serves as the low-temperature heat  
146 source and the TES tank 2 (15) serves as the high-temperature heat source. When the system  
147 provides hot water, the mains cold water flows into the TES tank 2. When the system is in  
148 operation for heating, the pump 4 (16) circulates the hot water in the TES tank 2 through the  
149 radiant floor (17).

150 Figure 2(b) shows the flow chart for control of the serial system operation. The room air  
151 temperature ( $T_{\text{room}}$ ), ambient air temperature ( $T_{\text{amb}}$ ), local solar irradiance ( $I$ ) as well as water  
152 temperatures at several locations such as the temperatures at the inlet and outlet of the solar  
153 collector ( $T_1$ ,  $T_2$ ), the temperature at the outlet of TES tank 1 to load ( $T_3$ ), hot water storage  
154 (HWS) temperature ( $T_{\text{HWS}}$ ) are measured/monitored for control of the serial system operation.  
155 The water temperature at the outlet of the evaporator ( $T_4$ ), the water temperatures at the inlet  
156 and outlet of the condenser ( $T_5$  and  $T_6$ ) and the temperature of the mains cold water supply ( $T_7$ )  
157 are measured/monitored for analysis of energy conservation of the heating system. Table 3  
158 gives the rule-based look-up table for control of the serial system operation.

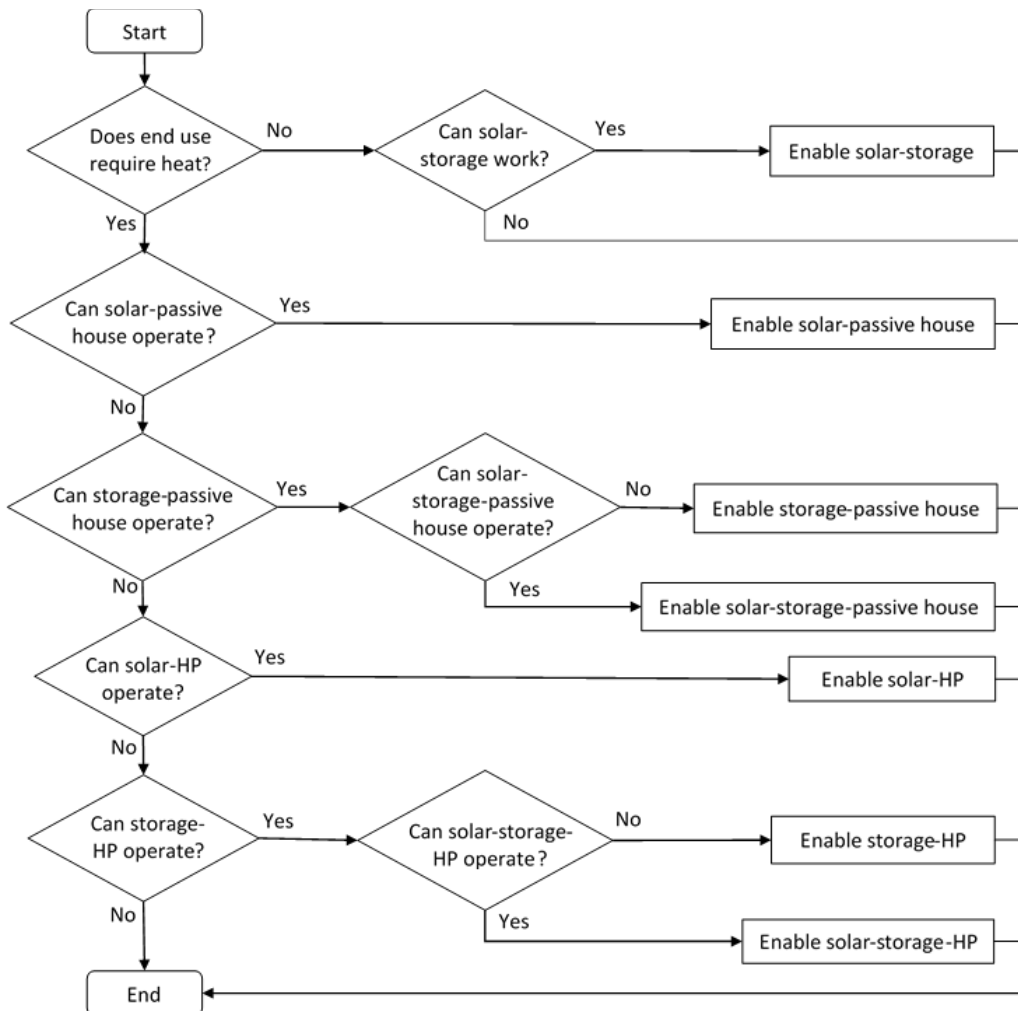
159





- 1: Solar collector    2, 6, 7, 13, 14: Valves    3: Pump 1    4: TES tank 1    5: Pump 2  
 8: Water-to-refrigerant evaporator    9: Compressor    10: Condenser  
 11: Expansion valve    12: Pump 3    15: TES tank 2    16: Pump 4    17: Radiant floor

a) Schematic of the serial system



b) Flow chart for system operation control

Figure 2: System and operation control of the serial IX-SAASHP

Table 3: The rule-based look-up table for control of the serial system operation

Operation mode	Temperature range (°C)	Pumps				Valves					SWHP
		3	5	12	16	2	6	7	13	14	
Collector- TES 1	$T_2 > T_3, T_{HWS} > 50$	O	X	X	X	O	X	X	X	X	X
Collector- TES 1- TES 2	$T_2 > T_3 > 50 > T_{HWS}$	O	O	X	X	O	O	O	X	O	X
Collector- TES 1- SWHP- TES 2	$T_2 > T_3, -5 < T_3 < 50, T_{HWS} < 50$	O	O	O	X	O	X	O	O	X	O
Collector- SWHP- TES 2	$T_2 < T_3, 50 > T_2 > -5, T_{HWS} < 50$	O	X	O	X	X	O	X	O	X	O
Collector- TES 2	$T_{HWS} < 50 < T_2 < T_3$	O	X	X	X	X	X	X	X	O	X
TES 1- TES 2	$T_3 > 50 > T_{HWS}$	X	O	X	X	X	O	O	X	O	X
TES 1- SWHP- TES 2	$-5 < T_3 < 50, T_{HWS} < 50$	X	O	O	X	X	X	O	O	X	O
SH: TES 2	$T_{room} < 18$	X	X	X	O	X	X	X	X	X	X
SH: Collector- TES 1	$T_2 > T_3, T_{HWS} > 50, T_{room} < 18$	O	X	X	O	O	X	X	X	X	X
SH: Collector- TES 1- TES 2	$T_2 > T_3, T_{HWS} < 50, T_{room} < 18$	O	O	X	O	O	O	O	X	O	X
SH: Collector- TES 1- SWHP- TES 2	$T_2 > T_3, -5 < T_3 < 50, T_{HWS} < 50, T_{room} < 18$	O	O	O	O	O	X	O	O	X	O
SH: Collector- SWHP- TES 2	$T_2 < T_3, 50 > T_2 > -5, T_{HWS} < 50, T_{room} < 18$	O	X	O	O	X	O	X	O	X	O
SH: Collector- TES 2	$T_{HWS} < 50 < T_2 < T_3, T_{room} < 18$	O	X	X	O	X	X	X	X	O	X
SH: TES 1- TES 2	$T_3 > 50 > T_{HWS}, T_{room} < 18$	X	O	X	O	X	O	O	X	O	X
SH: TES 1- SWHP - TES 2	$-5 < T_3 < 50, T_{HWS} < 50, T_{room} < 18$	X	O	O	O	X	X	O	O	X	O

168 Note: Collector: Solar collector. TES 1: Water TES tank1. TES 2: Water TES tank 2.

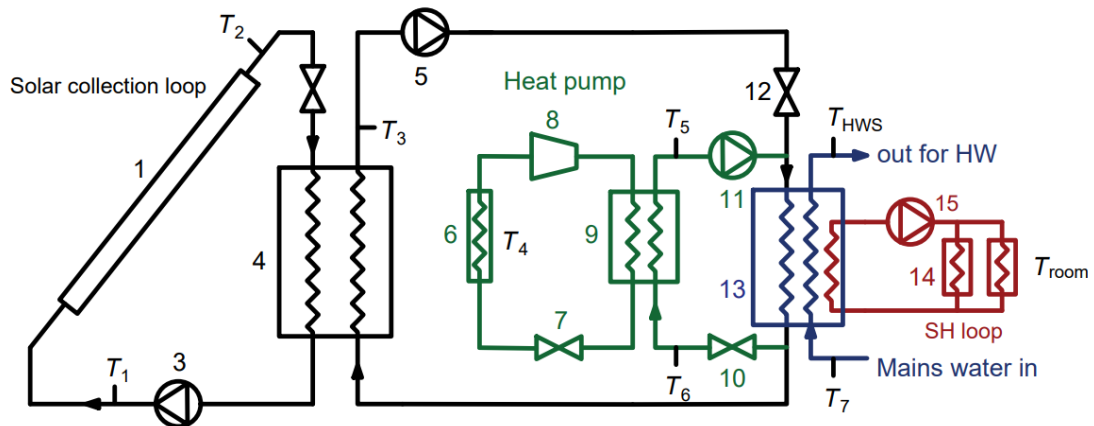
169 O: Pumps and SWHP are in operation; Valves is open. X: Pumps and SWHP are not in operation; Valves are closed.

171 3.2 Parallel system

172 Figure 3 shows a parallel IX-SAASHP, which consists of a solar collection loop (in black),  
 173 an ASHP unit (in green), a HW loop (in blue) and an SH loop (in red). The thermal energy is  
 174 stored in the TES tank 1 (valve 2 open) and circulated to TES tank 2 by pump 2 (valve 12  
 175 open). The ASHP consists of an air-to-refrigerant evaporator (6), an expansion valve(7), a  
 176 compressor (8) and a condenser (9). When the ASHP is in operation, the ambient air serves as  
 177 the low-temperature heat source.

178 Figure 3(b) shows the flow chart for control of the parallel system operation. Compared  
 179 with the serial system, the same temperatures are measured/monitored for control of the parallel  
 180 system operation. The air temperature at the outlet of the evaporator ( $T_4$ ), the water  
 181 temperatures at the inlet and outlet of the condenser ( $T_5$  and  $T_6$ ) and the temperature of the  
 182 mains cold water supply ( $T_7$ ) are measured/monitored for analysis of energy conservation of  
 183 the heating system. Table 4 gives the rule-based look-up table for control of the parallel system  
 184 operation.

185



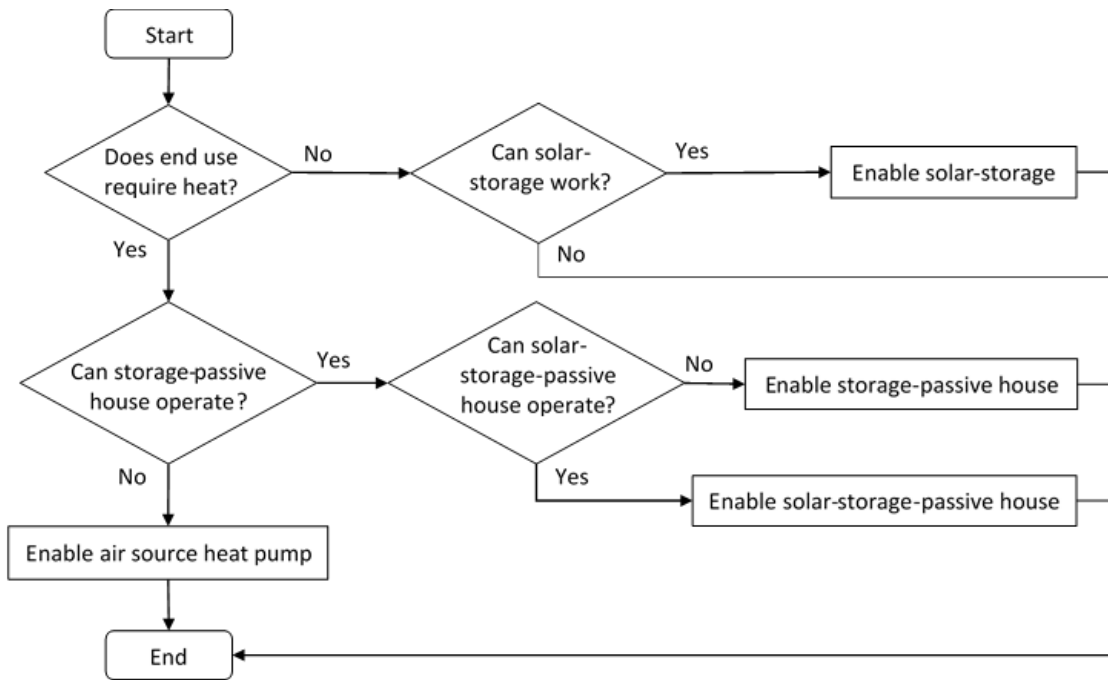
186

- 187 1: Solar collector    2, 10, 12: Valves    3: Pump 1    4: TES tank 1    5: Pump 2  
 188 6: Air-to-refrigerant evaporator    7: Expansion valve    8: Compressor  
 189 9: Condenser    11: Pump 3    13: TES tank 2    14: Radiant floor    15: Pump 4

190

191 a) Schematic of parallel system

192



b) Flow chart for system operation control

193  
194  
195  
196

Figure 3: System and operation control of the parallel IX-SAASHP

197

Table 4: The rule-based look-up table for control of the parallel system operation

198

199

200

201

202

203

204

205

206

207

208

Operation mode	Temperature range (°C)	Pumps				Valves			ASHP
		3	5	11	15	2	10	12	
Collector- TES 1	$T_2 > T_3, T_{HWS} > 50$	O	X	X	X	O	X	X	X
Collector- TES 1- TES 2	$T_2 > T_3 > 50 > T_{HWS}$	O	O	X	X	X	X	O	X
ASHP- TES 2	$T_3 < 50, T_{HWS} < 50$	X	X	O	X	X	O	X	O
TES 1- TES 2	$T_3 > 50 > T_{HWS}$	X	O	X	X	X	X	O	X
SH: TES 2	$T_{room} < 18$	X	X	X	O	X	X	X	X
SH: Collector- TES 1	$T_2 > T_3, T_{HWS} > 50, T_{room} < 18$	O	X	X	O	O	X	X	X
SH: Collector- TES 1- TES 2	$T_2 > T_3 > 50 > T_{HWS}, T_{room} < 18$	O	O	X	O	X	X	O	X
SH: ASHP- TES 2	$T_3 < 50, T_{HWS} < 50, T_{room} < 18$	X	X	O	O	X	O	X	O
SH: TES1- TES 2	$T_3 > 50 > T_{HWS}, T_{room} < 18$	X	O	X	O	X	X	O	X

Note: Collector: Solar collector. TES 1: Water TES tank1. TES 2: Water TES tank 2.

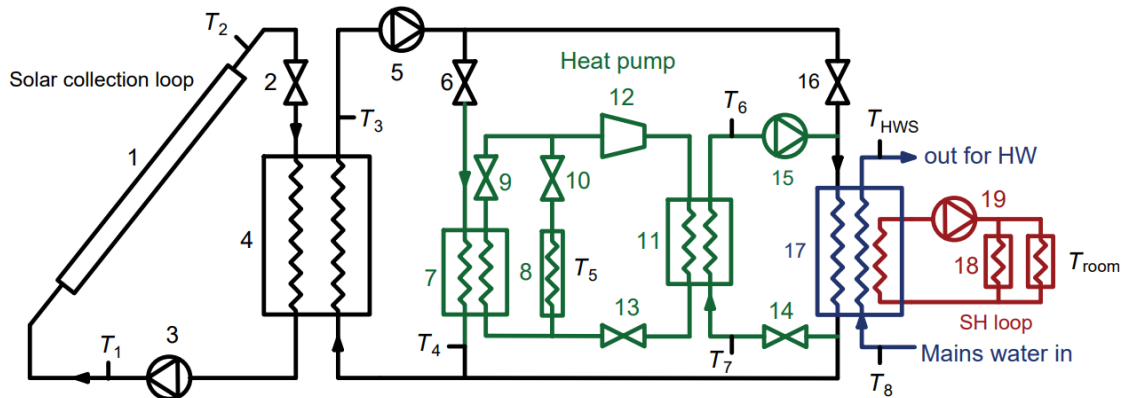
O: Pumps and ASHP are in operation; Valves is open. X: Pumps and ASHP are not in operation; Valves are closed.

209 3.3 Dual-source system

210 Figure 4 shows a dual-source IX-SAASHP, which consists of a solar collection loop (in  
 211 black), a SW-ASHP unit (in green), a HW loop (in blue) and an SH loop (in red). The SW-  
 212 ASHP consists of a water-to-refrigerant evaporator (7), an air-to-refrigerant evaporator (8), a  
 213 condenser (11), a compressor (12), and an expansion valve (13). When the SWHP is in  
 214 operation, the TES tank 1 (4) serves as the low-temperature heat source. When the ASHP is in  
 215 operation, the ambient air serves as the low-temperature heat source.

216 Figure 4(b) shows the flow chart for control of the dual-source system operation.  
 217 Compared with the serial and parallel systems, the same temperatures are measured/monitored  
 218 for control of the dual-source system operation. The water and air temperatures at the outlet of  
 219 the evaporator ( $T_4$  and  $T_5$ ), the water temperatures at the inlet and outlet of the condenser ( $T_6$   
 220 and  $T_7$ ) and the temperature of the mains cold water supply ( $T_8$ ) are measured/monitored for  
 221 analysis of energy conservation of the heating system. Table 5 gives the rule-based look-up  
 222 table for control of the dual-source system operation.

223



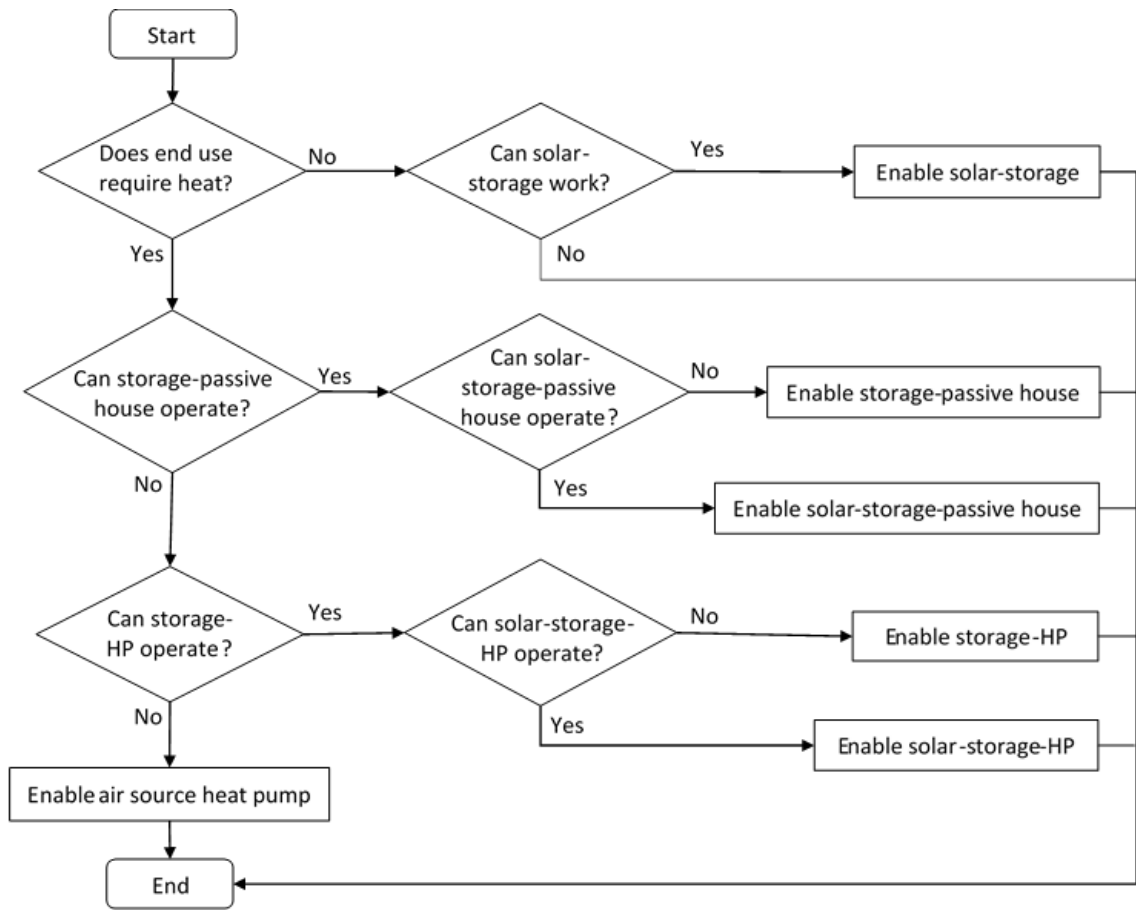
224

- |                                    |                             |                     |                                  |           |
|------------------------------------|-----------------------------|---------------------|----------------------------------|-----------|
| 1: Solar collector                 | 2, 6, 9, 10, 14, 16: Valves | 3: Pump 1           | 4: TES tank 1                    | 5: Pump 2 |
| 7: Water-to-refrigerant evaporator |                             |                     | 8: Air-to-refrigerant evaporator |           |
| 11: Condenser                      | 12: Compressor              | 13: Expansion valve | 15: Pump 3                       |           |
| 17: TES tank 2                     | 18: Radiant floor           | 19: Pump 4          |                                  |           |

225

a) Schematic of dual-source system

226



227

228

229

230

b) Flow chart for system operation control

Figure 4: System and operation control of the dual-source IX-SAASHP

Table 5: The rule-based look-up table for control of the dual-source system operation

Operation mode	Temperature range (°C)	Pumps				Valves						ASHP	SWHP
		3	5	15	19	2	6	9	10	14	16		
Collector- TES 1	$T_2 > T_3, T_{HWS} > 50$	O	X	X	X	O	X	X	X	X	X	X	X
Collector- TES 1- TES 2	$T_2 > T_3 > 50 > T_{HWS}$	O	O	X	X	O	X	X	X	X	O	X	X
Collector- TES 1- SWHP- TES 2	$T_2 > T_3, T_{amb} < T_3 < 50, T_{HWS} < 50$	O	O	O	X	O	O	O	X	O	X	X	O
ASHP- TES 2	$T_{amb} > T_3, T_{HWS} < 50$	X	X	O	X	X	X	X	O	O	X	O	X
TES 1- TES 2	$T_3 > 50 > T_{HWS}$	X	O	X	X	X	X	X	X	X	O	X	X
TES 1- SWHP- TES 2	$T_{amb} < T_3 < 50, T_{HWS} < 50$	X	O	O	X	X	O	O	X	O	X	X	O
SH: TES 2	$T_{room} < 18$	X	X	X	O	X	X	X	X	X	X	X	X
SH: Collector- TES 1	$T_2 > T_3, T_{HWS} > 50, T_{room} < 18$	O	X	X	O	O	X	X	X	X	X	X	X
SH: Collector- TES 1- TES 2	$T_2 > T_3 > 50 > T_{HWS}, T_{room} < 18$	O	O	X	O	O	X	X	X	X	O	X	X
SH: Collector- TES 1- SWHP- TES 2	$T_2 > T_3, T_{amb} < T_3 < 50, T_{HWS} < 50, T_{room} < 18$	O	O	O	O	O	O	O	X	O	X	X	O
SH: ASHP- TES 2	$T_{amb} > T_3, T_{HWS} < 50, T_{room} < 18$	X	X	O	O	X	X	X	O	O	X	O	X
SH: TES 1- TES 2	$T_3 > 50 > T_{HWS}, T_{room} < 18$	X	O	X	O	X	X	X	X	X	O	X	X
SH: TES 1- SWHP- TES 2	$T_{amb} < T_3 < 50, T_{HWS} < 50, T_{room} < 18$	X	O	O	O	X	O	O	X	O	X	X	O

232 Note: Collector: Solar collector. TES 1: Water TES tank1. TES 2: Water TES tank 2.

233 O: Pumps, SWHP and ASHP are in operation; Valves is open. X: Pumps, SWHP and ASHP are not in operation; Valves are closed.



#### 234 4. Modelling and simulation methods

235 TRNSYS 17 is used for the simulations. The working conditions of the systems, selection  
236 of TRNSYS modules and simulation schemes are described below.

##### 237 4.1 Working conditions

238 The systems are designed to provide SH and HW for the building over a year. The  $T_{\text{room}}$   
239 for thermal comfort is set to be 18 °C – 22 °C in the heating season. In the HP heating mode,  
240 the water temperature in the TES tank 2 is controlled to be not lower than 50 °C [22]. Four  
241 fifteen-minute water draws per day at a rate of 300 kg/h are used to represent typical low flow  
242 showers at 6 a.m., 8 a.m., 8 p.m., and 10 p.m. every day. To avoid scalding, the hot water  
243 supply temperature is set at 40 °C [23], which is supplied by mixing the stored hot water and  
244 mains water at the outlet of the hot water tank. For safe operation of the system, in the SHW  
245 operation mode, the maximum HWS temperature is controlled to be 80 °C.

246

##### 247 4.2 Selection of TRNSYS modules

248 Since flat plate solar collectors occupy about half of the current market share [7], the flat  
249 plate solar collector is selected as the solar collector. Solar collector module of Type 1b in  
250 TRNSYS is chosen to model this type of solar collector. To investigate the performances of  
251 the configurations of the three systems, auxiliary heater is not used and the demanded thermal  
252 energy is fully provided by the HPs and SHW. If the heat provided by the heating system is  
253 insufficient, the HWS temperature will be lower than the temperature set and the room air  
254 temperature will fall to below the temperature set for thermal comfort.

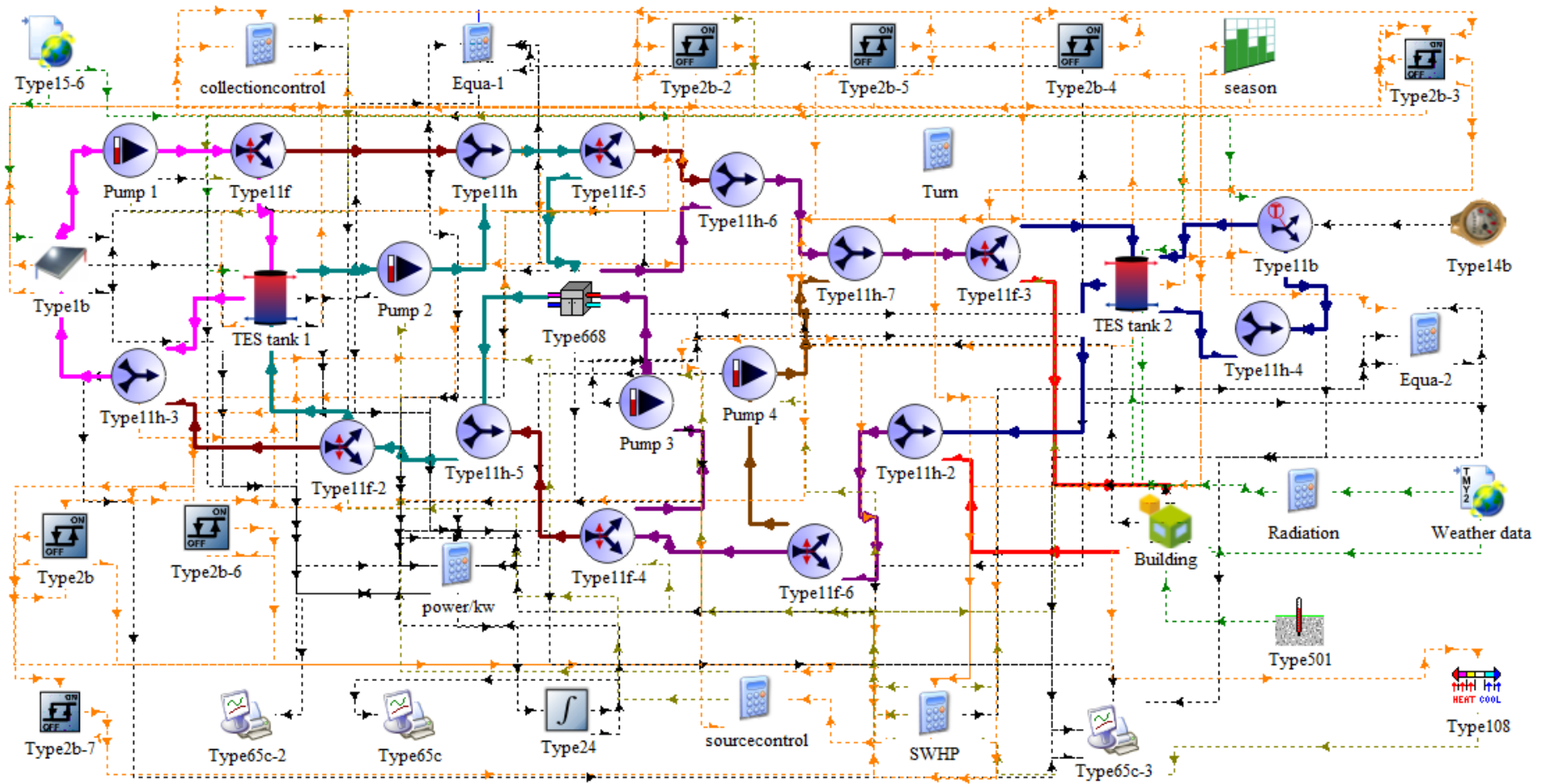
255 The sizing of the system is based on the demands of SH and HW. To meet the demands,  
256 different systems have different sizes of components. Since the serial system uses thermal  
257 energy collected by solar collector as the sole heat source, the required solar collector area is  
258 large to be 45 m<sup>2</sup> and the required size of water TES tank is large to be 3 m<sup>3</sup>. Since the parallel  
259 and dual-source systems have ASHP for compensation at low solar energy availability, the  
260 required sizes of solar collector and water TES tank are much smaller, 18 m<sup>2</sup> and 500 L,  
261 respectively, to ensure SHW temperature to be higher than 40 °C in non-heating seasons. When  
262 the SHW temperature is below 50 °C in non-heating seasons, the HP operates to ensure the  
263 HWS temperature in the safe range to inhibit bacteria.

264 All the HPs are set at a heating capacity of 8 kW. In the models of serial and dual-source  
265 IX-SAASHPs, the SWHP module (Type 668) is modified based on sample file of 30HXC-HP2  
266 from Carrier United Technologies. In the models of the parallel and dual-source IX-SAASHPs,  
267 the ASHP module (Type 941) is modified based on the sample file of YVAS012, York, Jonson

268 Control. Note that the ASHP module (Type 941) available in TRNSYS does not consider the  
269 frosting and defrosting and their effects on the ASHP performance. It is anticipated that the  
270 results provide deep understanding for application potential of SAASHPs in high latitude  
271 regions. In the model of dual-source IX-SAASHP, the dual-source HP is simulated by  
272 combining a SWHP (Type 668) and an ASHP (Type 941). TRNSYS modules selected for  
273 modelling the components of the three systems and relevant parameters are listed in table 6.  
274 Figure 5 shows the TRNSYS models and control functions for serial, parallel and dual-source  
275 IX-SAASHPs. The solid lines stand for the pipe connections, and the dot lines stand for the  
276 control connections.

Table 6: TRNSYS modules selected for modelling the components of the three systems and relevant parameters

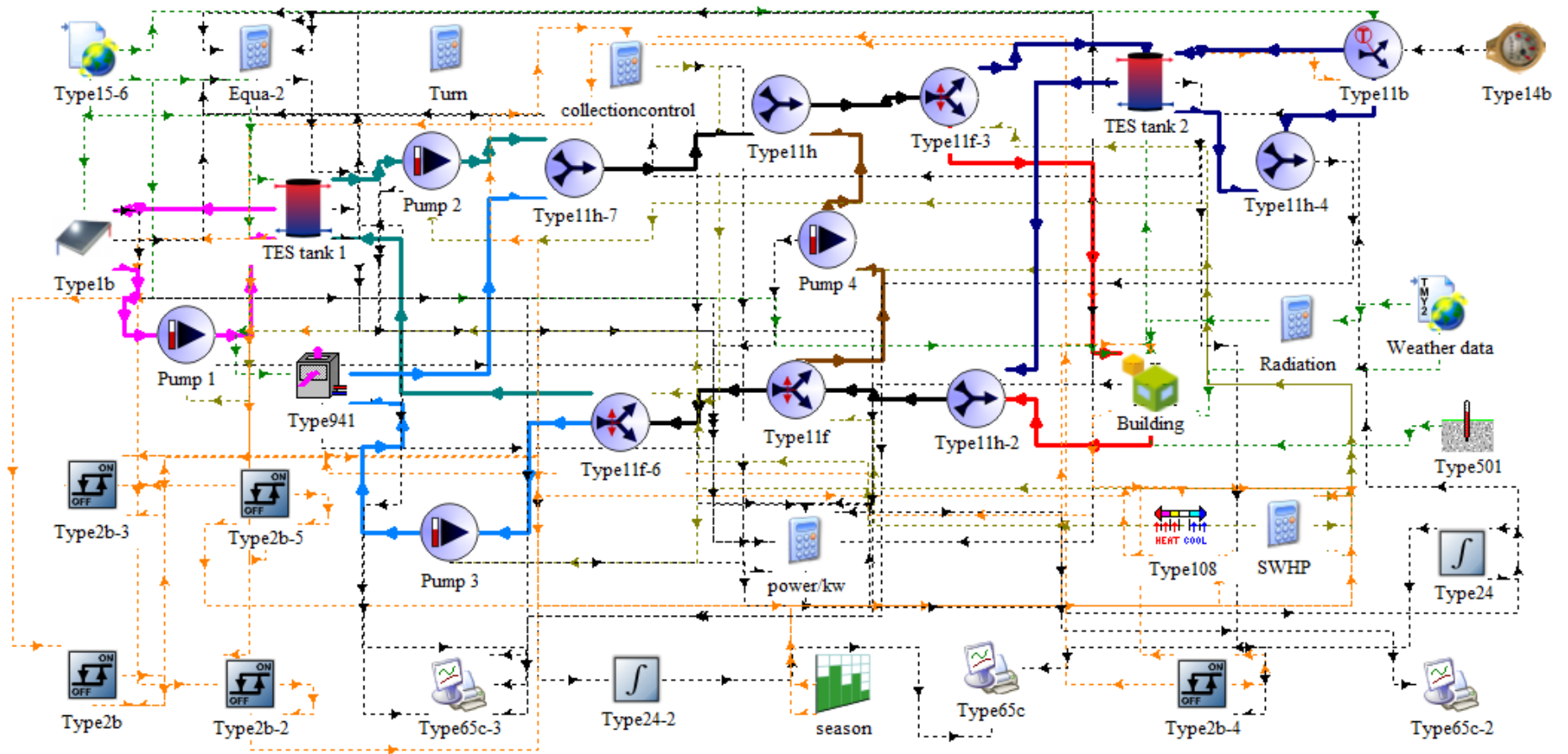
Component	Module	System	Parameter	Value
<b>Solar collector</b>	Type 1b	Serial system	Area	45 m <sup>2</sup>
		Parallel and dual-source systems	Area	18 m <sup>2</sup>
			Inclination angle	51.5°
		All systems	Tested flow rate	30 kg/hm <sup>2</sup>
			Intercept efficiency	0.8
			Efficiency slope	13 kJ/hm <sup>2</sup> k
			Efficiency curvature	0 kJ/hm <sup>2</sup> k <sup>2</sup>
			1 <sup>st</sup> order IAM	0.2
2 <sup>nd</sup> order IAM	0			
<b>TES tank 1</b>	Type 4a	All systems	Heat loss coefficient	0.2 W/(m <sup>2</sup> K)
		Serial system	Volume	3000 L
			Height	2.15 m
		Parallel and dual-source systems	Volume	500 L
			Height	1.175 m
<b>TES tank 2</b>	Type 4a	All systems	Heat loss coefficient	0.2 W/(m <sup>2</sup> K)
			Volume	300 L
			height	1 m
<b>ASHP</b>	Type 941	Parallel and dual-source systems	Blower power	0.15 kW
			Total air flow rate	1500 l/s
			User defined file	YVAS012, York, Jonson Control
<b>SWHP</b>	Type 668	Serial and dual-source systems	User defined file	30HXC-HP2, Carrier United Technologies
<b>Pump 1</b>	Type 110	All systems	Rated flow rate	500 kg/h
			Rated power	30 W
<b>Pump 2</b>	Type 110	All systems	Rated flow rate	800 kg/h
			Rated power	50 W
<b>Pump 4</b>	Type 110	All systems	Rated flow rate	800 kg/h
			Rated power	50 W
<b>Pump in SWHP loop</b>	Type 110	Serial and dual-source systems	Rated flow rate	870 kg/h
			Rated power	50 W
<b>Pump in ASHP loop</b>	Type 110	Parallel and dual-source systems	Rated flow rate	870 kg/h
			Rated power	50 W



280

281

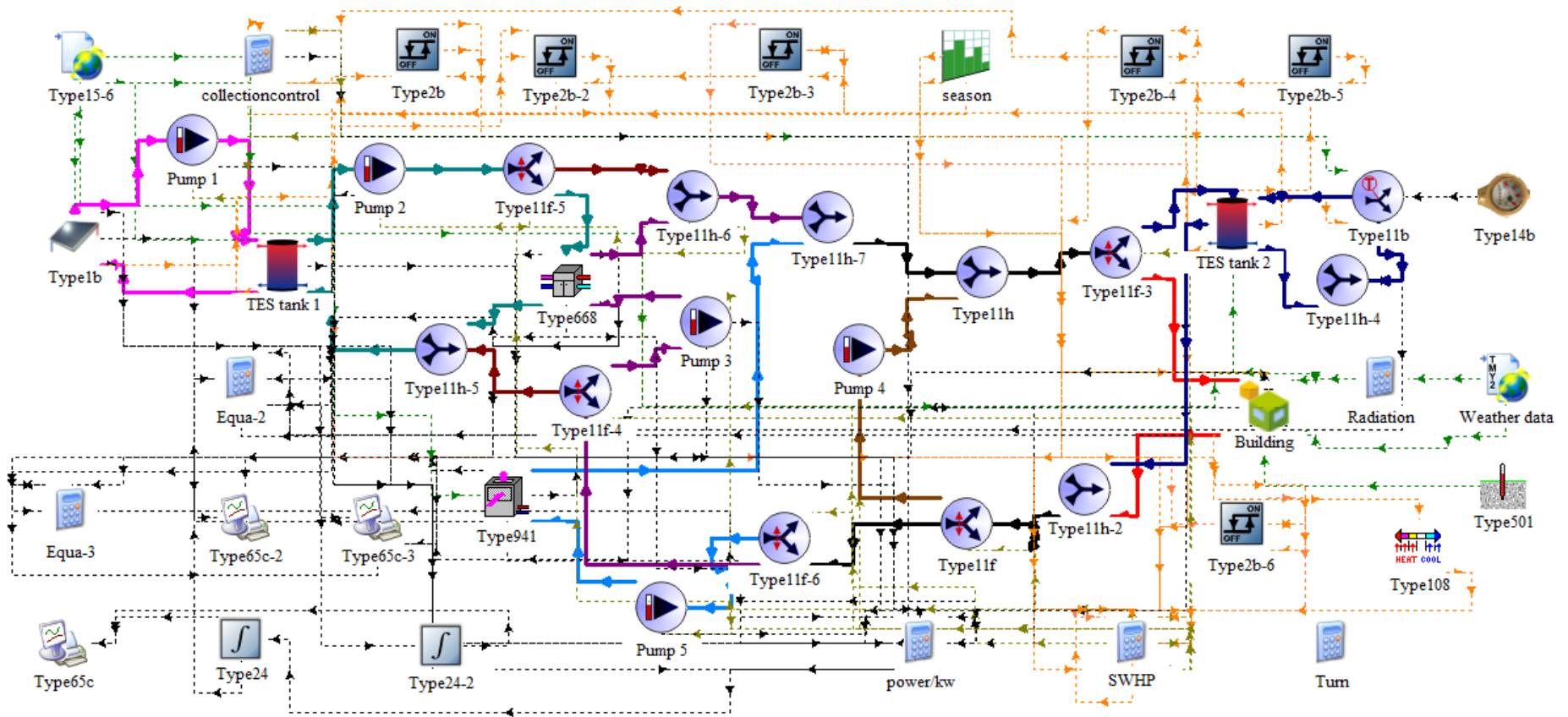
a) Serial IX-SAASHP



b) Parallel IX-SAASHP

282

283



c) Dual-source IX-SAASHP

284

285

286

287

Figure 5: TRNSYS models and control functions for serial, parallel and dual-source IX-SAASHPs.

288

(Solid lines: pink - solar collector- TES tank 1 loop; dark red - bypass; green - TES tank 1-SWHP loop; purple - SWHP loop; light blue - ASHP loop; black -

289

user side loop; brown - TES tank 2-radiant floor loop; red - SH loop; dark blue - HW loop). (Dot lines: orange - monitored parameters; sage green - control

290

signals; dark green - weather parameters; black - data outputs).

291 4.3 Simulation scheme

292 The operation period is set at one year with a time step of 0.0167 h. The systems start to  
293 operate from the middle of the year (4380 h) with an initial water temperature of 13.4 °C in the  
294 TES tanks, which is the water temperature of mains water supply.

295

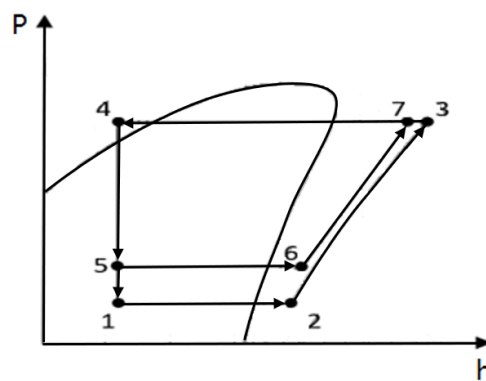
296 **5. Evaluation of performance**

297 The three IX-SAASHPs have different system configurations. They all include a vapour-  
298 compression cycle HP. Their performance can be evaluated by the performance indicators.

299 5.1 Thermodynamics cycle of the heat pumps

300 Figure 6 shows the ideal vapour-compression cycles of the ASHP (1-2-3-4-1) and SWHP  
301 (5-6-7-4-5) on  $P-h$  diagram. The degree of superheat of the refrigerant vapour entering the  
302 compressor is taken to be the same for both HPs. The flow resistance on the refrigerant side in  
303 both evaporator and condenser is neglected.

304



305

306 Figure 6:  $P-h$  diagram of ideal vapour-compression cycle HPs

307

308 5.2 System performance indicators

309 The performance of the heating systems is evaluated by a variety of indicators including  
310 the room air temperature, HWS temperature,  $SPF$  of the system ( $SPF_{sys}$ ),  $SPF$  of the HP  
311 ( $SPF_{HP}$ ),  $COP$  of the HP module, and the solar fraction ( $SF$ ). The room air temperature is an  
312 indication whether the heat provision by the heating system meets the **heat** demand of the  
313 building. The measured room air temperature is also the quantity that determines the on/off  
314 operation of the heating system. The HWS temperature indicates the amount of thermal energy  
315 stored in the TES tanks and also determines the on/off operation of the SWHP. The  $SPF_{sys}$   
316 describes the overall performance of the whole heating system over the heating season of the  
317 year and is defined by Eq. (1):

318 
$$SPF_{sys} = \frac{\int (Q_{SH} + Q_{HW}) \times dt}{\int W_{tot} \times dt} \quad (1)$$

319 where  $Q_{SH}$  and  $Q_{HW}$  are the thermal energies supplied by the system for SH and HW,  
 320 respectively, and  $W_{tot}$  is the total electricity consumed by the HP and all water pumps given by  
 321 Eq. (2):

322 
$$W_{tot} = W_{HP} + W_{pumps} \quad (2)$$

323 where  $W_{HP}$  is the electricity consumed by the HP calculated by Eq. (3):

324 
$$W_{HP} = j_{ASHP} W_{ASHP} + j_{SWHP} W_{SWHP} \quad (3)$$

325 where  $W_{ASHP}$  and  $W_{SWHP}$  are the electricity consumed by the ASHP and SWHP, respectively,  
 326  $j_{ASHP}$  and  $j_{SWHP}$  have values either 1 or 0 representing on or off operation status of ASHP and  
 327 SWHP. For serial system,  $j_{ASHP} = 0$  and  $j_{SWHP} = 1$ . For parallel system,  $j_{ASHP} = 1$  and  $j_{SWHP} = 0$ .  
 328 For dual-source system,  $j_{ASHP}$  and  $j_{SWHP}$  can be 1 or 0, depending on their on/off operation  
 329 status.

330 The  $SPF_{HP}$  describes the overall performance of a HP over the heating season and is  
 331 defined by Eq. (4):

332 
$$SPF_{HP} = \frac{\int Q_{HP,con} \times dt}{\int W_{HP} \times dt} \quad (4)$$

333 where  $Q_{HP,con}$  is the heat transferred from the condenser of the HP to water circulating to TES  
 334 tank 2, given by Eq. (5):

335 
$$Q_{HP,con} = j_{ASHP} Q_{ASHP,con} + j_{SWHP} Q_{SWHP,con} \quad (5)$$

336 where  $Q_{ASHP,con}$  and  $Q_{SWHP,con}$  are the heat transferred from the condenser of ASHP and SWHP  
 337 to water circulating to TES tank 2, respectively.

338 The  $COP$  of the HP is defined by Eq. (6):

339 
$$COP = Q_{HP,con} / W_{HP} \quad (6)$$

340 The  $SF$  of the heating system, the contribution ratio of the solar thermal energy collected  
 341 to the system **heat** provision over the heating season, is defined by Eq. (7):

342 
$$SF = 1 - \frac{\int (Q_{ASHP,con} + W_{SWHP}) \times dt}{\int (Q_{HW} + Q_{SH}) \times dt} \quad (7)$$

## 343 6. Results and discussions

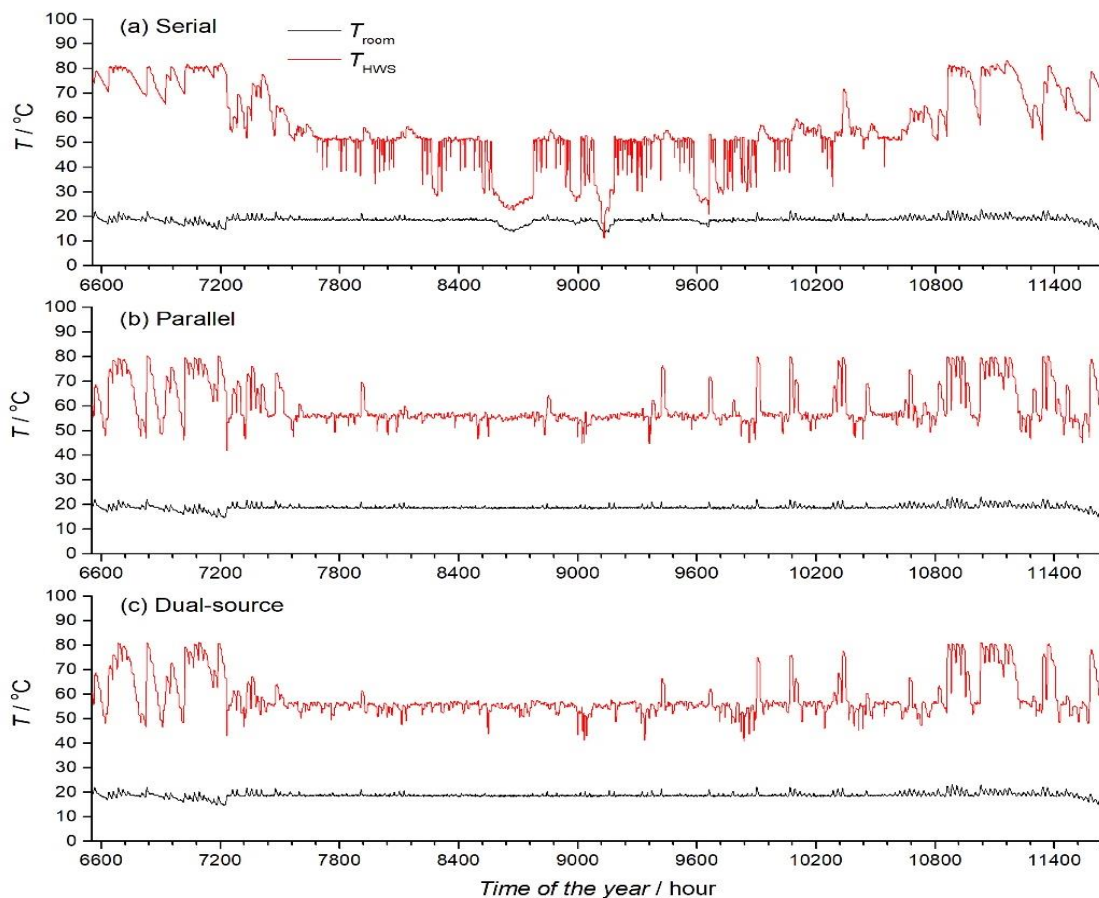
344 Based on the three IX-SAASHPs, the models in TRNSYS are established. Simulations  
 345 are performed and the system performances are then obtained.

### 346 6.1 Seasonally heating performance

347 Figure 7 shows the variations of the room air temperature ( $T_{room}$ , the black line) and the  
 348 HWS temperature ( $T_{HWS}$ , the red line) over the heating season for serial, parallel and dual-  
 349 source IX-SAASHPs. It is seen that the HWS temperature may suddenly drop to below 50 °C



350 because after water draws, feedwater enters the hot water tank. However, the IX-SAASHPs  
 351 respond quickly to lift the HWS temperature to above 50 °C. From Fig.7(a), it is seen that, the  
 352 serial IX-SAASHP cannot meet the **heat** demand in winter; in some cases the room air  
 353 temperature is below 18 °C. The lowest room air temperature is 13.4 °C and the lowest HWS  
 354 temperature of 11.3 °C. The lowest water temperature at the outlet of the evaporator is -7.1 °C.  
 355 This is still within the safe operation range of the system according to the operation introduction  
 356 of the 30HXC-HP2 of Carrier United Technologies.  
 357



358  
 359 Figure 7: Variations of room air temperature and HW temperature at the outlet of TES tank 2 for three  
 360 systems over a heating season

361 During the simulation of serial IX-SAASHP, to improve the heating capacity in winter,  
 362 larger collector areas, collectors with better efficiencies and larger storage tanks have been tried.  
 363 It was found that heating capacity is mainly limited by solar irradiation intensity, rather than  
 364 component parameters. Improving collector area and efficiency can hardly enhance system  
 365 performance. For example, when a solar collector of 48 m<sup>2</sup> is used, the lowest room temperature  
 366 and HWS temperature are almost the same, 13.5 °C and 11.5 °C, respectively. When a solar  
 367 collector with an intercept efficiency of 0.85 is used, the lowest room temperature and HWS

368 temperature are almost the same, 13.7 °C and 11.5 °C, respectively. The use of a larger TES  
369 tank 1 increases the capacity of TES, but may reduce its water temperature i.e. the heat source  
370 temperature for SWHP, resulting in lower heat provision of the system. When a TES tank 1 of  
371 3.5 m<sup>3</sup> is used, the lowest HWS temperature is almost the same at 11.4 °C, but the lowest HWS  
372 temperature occurs 4 times in winter. In addition, the lowest room air temperature drops even  
373 to 11.8 °C.

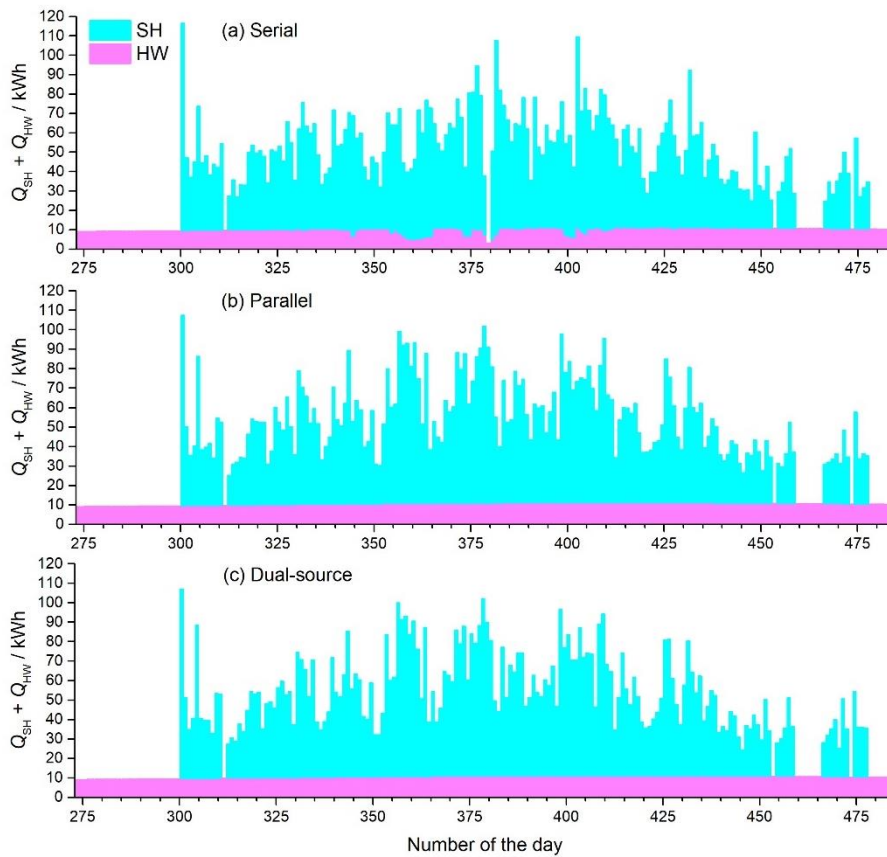
374 As shown in Figure 7 (b) and (c), the use of ASHP make the system meet the **heat** demands  
375 well. The lowest water temperature at the outlet of the SWHP evaporator is about -5 °C and the  
376 air temperatures at the outlet of the ASHP evaporator are also about -5 °C. This ensures the  
377 safe operation of SWHP and ASHP over the heating season.

378

## 379 6.2 Daily heat provision

380 Figure 8 shows the variations of daily heat provision (kWh) for SH and HW for three  
381 systems over a heating season. The blue column represents the daily heat provision for SH and  
382 the pink column represents that for HW. The columns are stacked to represent the total heat  
383 provision. It can be seen that the **heat provision for space heating is mainly required** in  
384 December to February. The parallel and the dual-source IX-SAASHPs have almost the same  
385 daily heat provision, higher than that of the serial IX-SAASHP. The largest daily heat provision  
386 from parallel and dual-source systems are around 100 kWh. At the same day, the serial system  
387 only provides thermal energy of 3.2 kWh. Especially, in December, the daily heat provision of  
388 the serial system is obviously lower than those of the other systems.

389

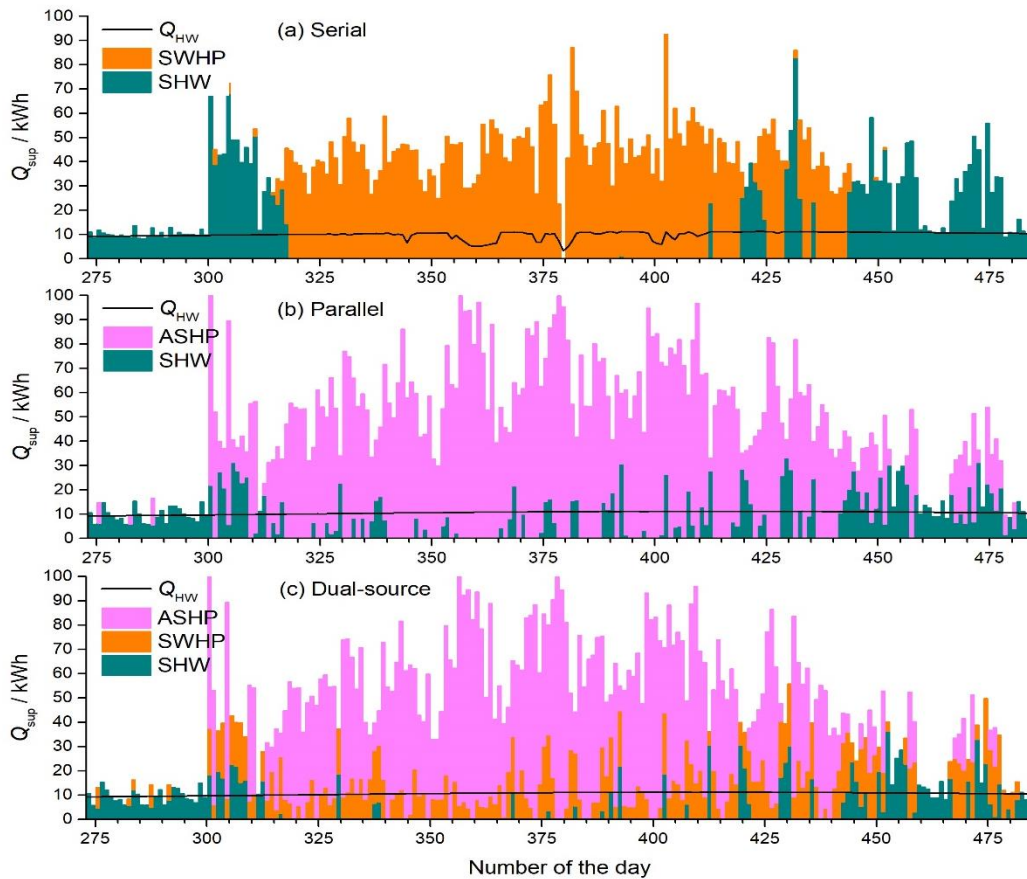


390

391 Figure 8: Variations of daily heat provision for SH and HW for three systems over a heating season

392

393 Figure 9 shows the variations of daily heat provision (kWh) supplied by direct SHW  
 394 (green), ASHP (red) and SWHP (orange) for three systems over a heating season. The columns  
 395 are stacked to represent the total daily heat provision. The black line refers to the daily HW  
 396 provision as a reference. The thermal energy loss and storage from the hot water tank is  
 397 included as a part of the daily heat provision. For the serial system, the use of solar energy as  
 398 the sole heat source providing heat either directly or by the SWHP may result in zero heat  
 399 provision e.g. on the 14<sup>th</sup> (379<sup>th</sup>) day. For the dual-source system, the large proportion of heat  
 400 is provided by the ASHP. This suggests the importance of employing ASHP in a heating system  
 401 for stable operation while the SWHP benefits to improve system performance.



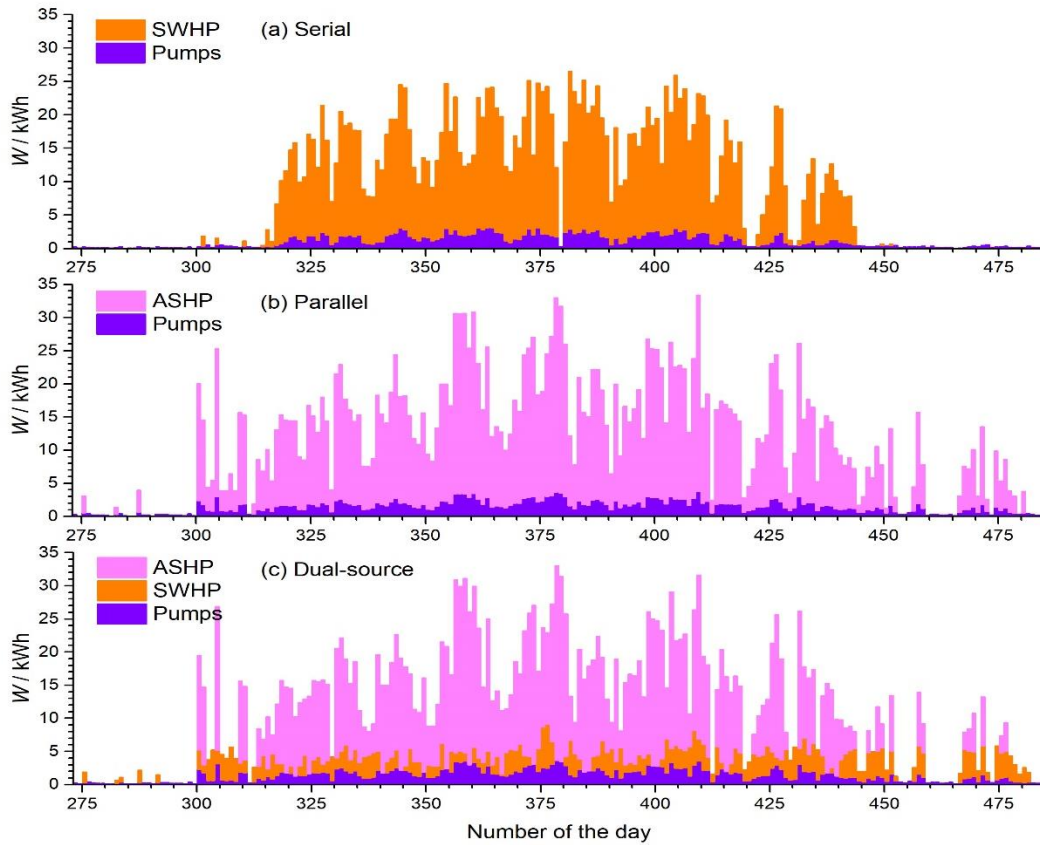
402

403 Figure 9: Variations of daily heat provision supplied by direct SHW, ASHP and SWHP for three  
 404 systems over a heating season

405

406 Figure 10 displays the variations of daily electricity consumed (kWh) by the systems over  
 407 a heating season. The red column is the electricity consumed by the ASHP, the orange column  
 408 is that by the SWHP and the purple column is that by the pumps. The columns are stacked to  
 409 represent the total electricity consumed by the system. In all systems, pumps are mainly used  
 410 to support HPs. The electricity consumed by the pumps in SHW periods is low, only around  
 411 0.1 - 0.4 kWh per day. Since parallel and dual-source systems have smaller solar collector and  
 412 storage tank, their solar utilisation is lower than that of serial system. Their electricity  
 413 consumption is thereby higher. The largest electricity consumption is around 32 kWh on the  
 414 14<sup>th</sup> day. However, considering the large scale of the serial system, its electricity consumption  
 415 is still relatively high. The largest electricity consumption is around 25 kWh a day because  
 416 serial IX-SAASHP requires more pumps during operation. This indicates that it is not feasible  
 417 to use solar thermal energy as the dominant heat source in London.

418



419

420

Figure 10: Variations of daily electricity consumed by the systems over a heating season

421

422

423

424

425

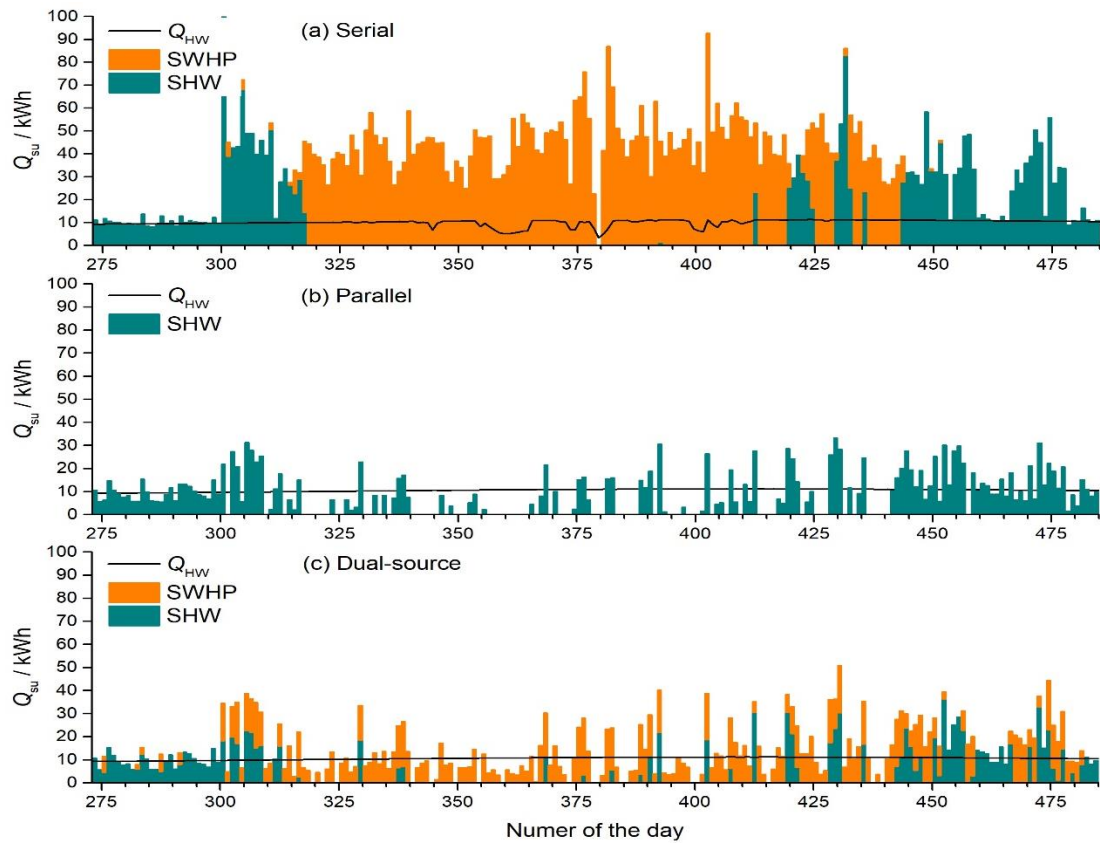
426

427

428

429

Figure 11 shows variations of daily solar thermal energy (kWh) used for SH and HW over a heating season. The green column is the solar thermal energy to SHW, and the orange column is that to SWHP. The columns are stacked to represent the total solar thermal energy collected in the system. The black line refers to the average daily HW provision for reference. In most days using SWHP, solar thermal energy mainly works as the heat source to the SWHP and that left for direct SHW is limited. Especially, for the serial system, the solar thermal energy is purely used for SWHP in winter.



430

431

Figure 11: Variations of daily solar thermal energy used for SH and HW over a heating season

432

433

434

435

436

437

438

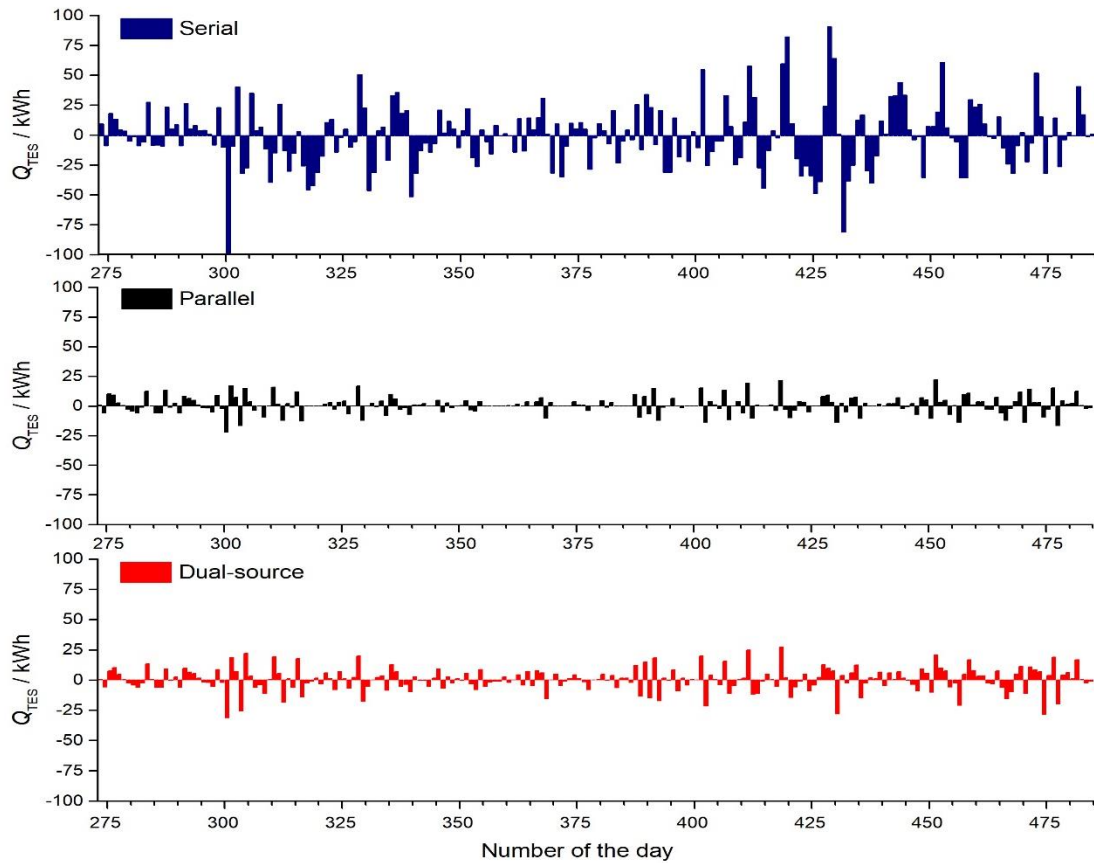
439

440

441

442

Figure 12 shows the variations of daily thermal energy storage ( $Q_{TES}$ ) in serial (blue), parallel (black) and dual-source (red) IX-SAASHPs over a heating season. Positive value refers to the thermal energy charged and negative value refers to the thermal energy discharged. Comparison between Figures 11 and 12 indicates that using SWHP increases the utilisations of solar thermal energy and the seasonal storage. For example, at the beginning of the heating period, in the serial system, the storage tank discharges around 100 kWh thermal energy stored in non-heating seasons. On the one hand, employing seasonal thermal storage can balance the seasonal difference between solar irradiance and **heat** demand, improving the system performance. On the other hand, large requirements on seasonal thermal storage imply insufficient solar availability in winter, impacting the stability of system operation.



443

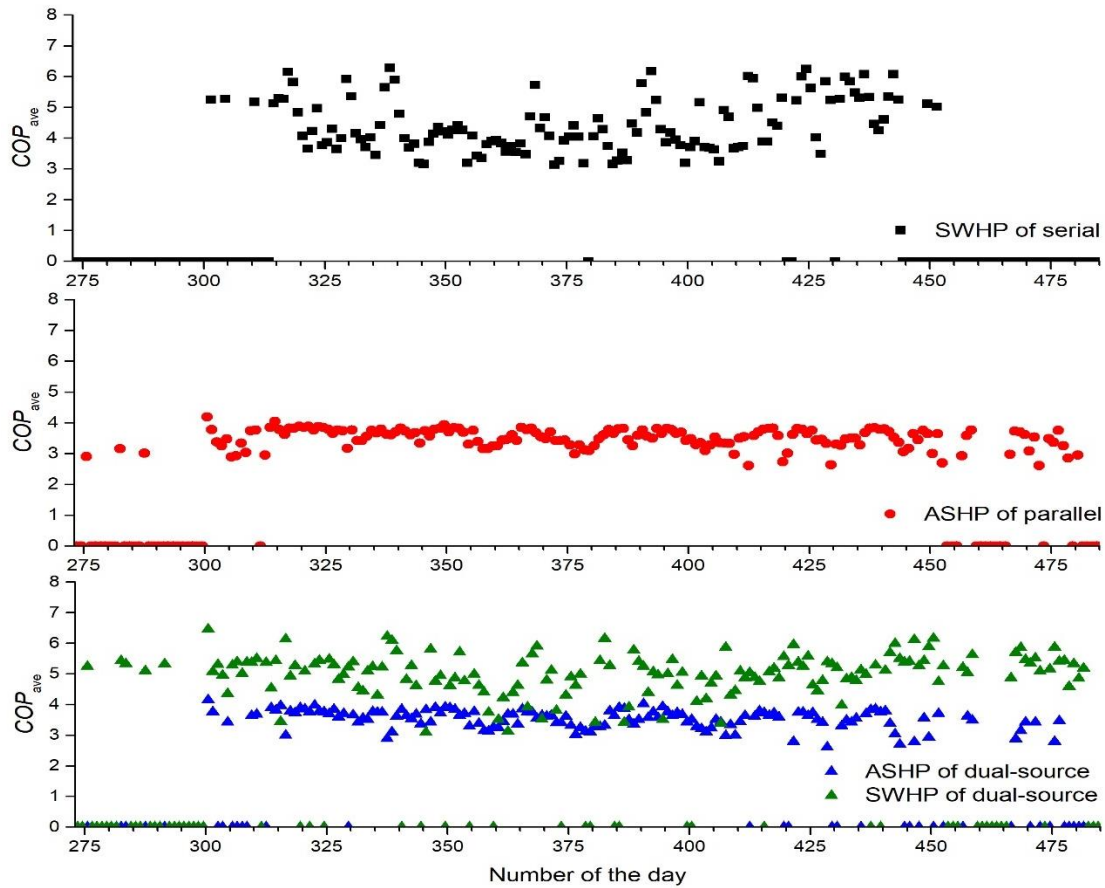
444

445 Figure 12: Variations of daily thermal energy storage ( $Q_{TES}$ ) over a heating season. Positive value  
 446 refers to the thermal energy charged and negative value refers to the thermal energy discharged.

447

### 448 6.3 Efficiencies of the heat pump module(s)

449 Figure 13 shows the variations of daily averaged  $COP$  of the HPs in three systems over a  
 450 heating season. The daily average  $COP$ s of the SWHP in serial system and the ASHP in parallel  
 451 system are in black and red, and those of the ASHP and SWHP of the dual-source IX-SAASHP  
 452 are in blue and green. It can be seen that, in the serial IX-SAASHP, the  $COP$  of the SWHP  
 453 module ranges from 3 to 7. Wherein, the  $COP$  ranges from 3 to 5 in most occasions. In the  
 454 parallel system, the  $COP$  of the ASHP module ranges from 2.5 to 4.5. Even though the serial  
 455 IX-SAASHP has higher  $COP$  of the HP module, according to previous analysis, it has low heat  
 456 provision due to the limits of weather conditions. In the dual-source IX-SAASHP, the  $COP$  of  
 457 the SWHP and ASHP modules are the same to those in serial and parallel system, ranging from  
 458 2.5 to 4.5 and from 3 to 7, respectively.



459

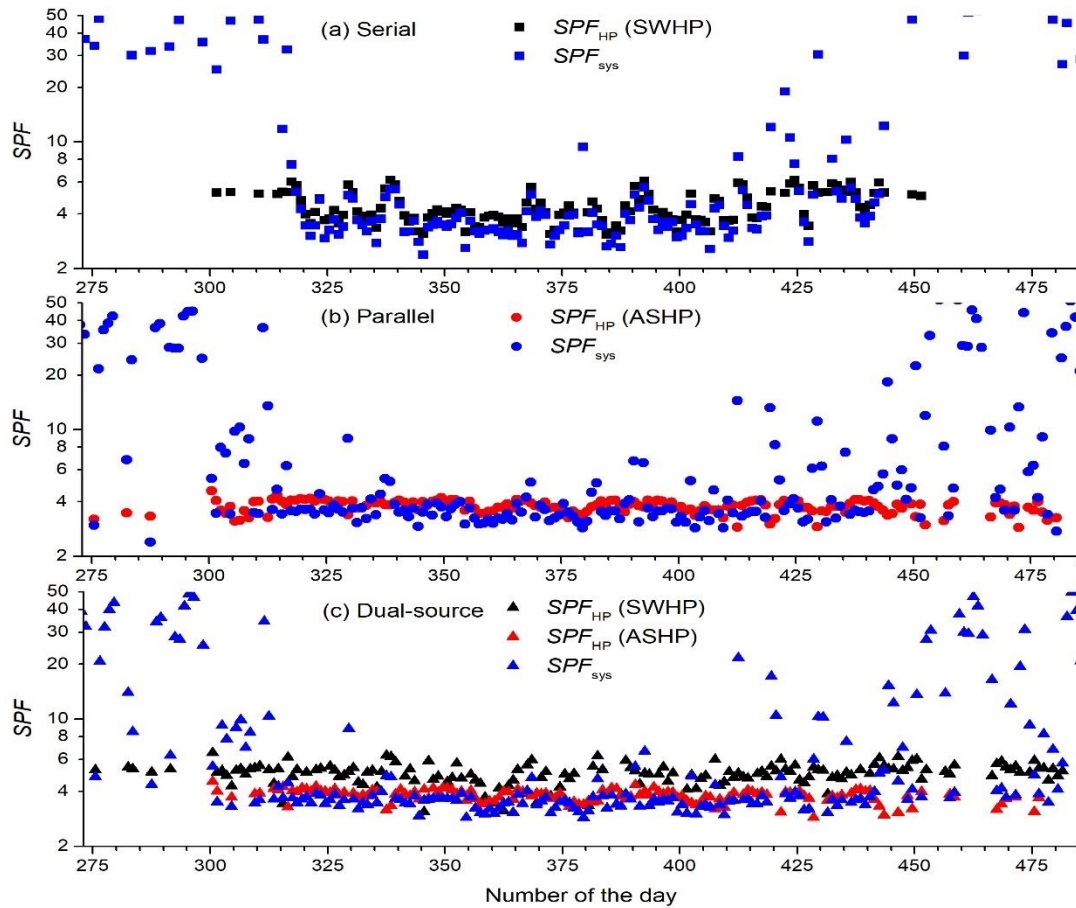
460

461 Figure 13: Variations of daily averaged  $COP$  of the HPs in three systems over a heating season.

462

463 Figure 14 shows the  $SPF_{sys}$  of the system (blue symbols) and  $SPF_{HP}$  of the HPs (black  
 464 symbol for SWHP and red symbols for ASHP) for three systems. In all **three** systems, the  
 465 lowest daily  $SPF_{HP}$  is 2.9-3.1. Considering the electricity consumed by pumps,  $SPF_{sys}$  is lower  
 466 than  $SPF_{HP}$  in HP dominant periods. The lowest daily  $SPF_{sys}$  of the serial and parallel systems  
 467 is 2.4 and that of the dual-source system is 2.9. All the lowest daily  $SPF_{sys}$  occur in December.





468

469

470

Figure 14: Variations of daily  $SPF_{sys}$  and  $SPF_{HP}$  over a heating season

471

#### 472 6.4 Yearly operation performance

473

The overall operation performances of the IX-SAASHPs are listed in table 7. The system simulation considers heat exchange with the ambient environment and the thermal energy stored in the tanks at the beginning and the ending.

474

475

Table 7: Overall operation performance of the IX-SAASHPs

	System	Period	Serial	Parallel	Dual-source
<b>Heat provision (kWh)</b>	HW	Heating season	2124.8	2235.2	2237.7
		Non-heating season	1427.3	1426.9	1427.5
	Total		7270.5	7523.7	7527.9
<b>Heat provision (kWh)</b>	SWHP		10822.6	11185.8	11193.1
	ASHP		7008.6	0	2289.1
	Solar	Heating season	0	8218.0	6586.6
		Non-heating season	2567.1	1802.6	1187.6
			1528.7	1444.1	1409.4
	SWHP		1705.7	0	449.2
	ASHP		0	2136.9	1737.7

<b>Electricity consumption (kWh)</b>	Water pumps	Heating season	233.2	304.7	295.0
		Non-heating season	27.8	42.7	40.7
	Total		1966.763	2511.3	2522.6
<b><math>SPF_{HP}</math></b>	SWHP		4.1	0	5.1
	ASHP		0	3.8	3.8
<b><math>COP_{ave}</math></b>	SWHP		4.5	0	5.0
	ASHP		0	3.5	3.5
<b>Solar thermal energy (kWh)</b>	To SWHP		5302.9	0	1839.9
	To end use	Heating season	2567.1	1802.6	1187.6
		Non-heating season	1528.7	1444.2	1409.4
	Total		9980.0	3593.2	4706.7
<b>Thermal energy from ambient air (kWh)</b>			0	6054.1	4848.9
<b><math>SF</math></b>	Heating season		83.8%	18.5%	31.0%
	Yearly		86.7%	29.0%	39.6%
<b><math>SPF_{sys}</math></b>	Heating season		4.9	4.0	3.9
	Yearly		5.5	4.5	4.4

477

478 All the IX-SAASHPs can obtain yearly  $SPF_{sys}$  above 4.4. Compared with the systems  
479 listed in table 1 [8-20], the simulated results show relatively good system performances. This  
480 suggests that, for the weather conditions in London, IX-SAASHPs can be a promising choice  
481 for SH and HW. It is interesting to note that, using the same area of solar collector and TES  
482 tank volume, the parallel system has a lower yearly  $SF$  (29%) than the dual-source system  
483 (39.6%), but both systems share the similar  $SPF_{sys}$ , 4.5 and 4.4. This means that in the dual-  
484 source system, the electricity consumed by pumps balances the electricity saved by using solar  
485 energy. In addition, it should be noticed that, though the dual-source IX-SAASHPs always  
486 have a  $COP$  under 3.5 in previous studies [7], for the weather conditions in London, the dual-  
487 source system can be comparable to the parallel system. This suggests that the dual-source IX-  
488 SAASHP is of higher application potential in high altitude regions.

489 For all the three systems, the space heating takes account of around 67% of the total heat  
490 demand. This suggests that, although SH takes a shorter period of time, it is more important  
491 than HW in domestic heating sector. To make the domestic heating sector greener, advanced  
492 technologies in various aspects helping reduce the heat demand for space heating, such as low  
493  $U$ -value materials and passive design, need to be developed.

494 In terms of heat provision, the HPs contribute to the most heat provision (around 83%)  
495 and also consume the most of the overall electricity consumption (around 85%). To increase  
496 heat provision and reduce operation cost, it is important to improve HP technologies for higher  
497  $COP$  such as using high efficient compressor, suitable refrigerant and heat exchangers with  
498 enhanced heat transfer and optimised design.

499

## 500 6.5 Economic analyses

501 To evaluate the economic performance of IX-SAASHPs, under net-zero target in the UK,  
502 economic analyses are conducted for IX-SAASHPs, electric water heater and gas boiler, as  
503 well as electric heater and gas boiler boosted SHW systems.

504 For economic analyses, the total energy consumption of the heating systems,  $Q_{tot}$ , is  
505 calculated by Eq. (8):

$$506 \quad Q_{tot} = (Q_{sh} + Q_{hw} - Q_{ce})/\eta \quad (8)$$

507 where  $Q_{ce}$  is the clean energy (extracted from solar and ambient air sources) used by the heating  
508 system and  $\eta$  is the efficiency of the electric water heater and gas boiler.

509 The payback period,  $P_{pb}$ , is defined on the basis of electric water heater by Eq. (9):

$$510 \quad P_{pb} = C_i / C_{spy} \quad (9)$$

511 where  $C_i$  is the initial cost difference and  $C_{spy}$  is the cost saving per year calculated by Eq.(10)  
512 and Eq.(11), respectively.

$$513 \quad C_i = C_{i0} - C_{ieh} \quad (10)$$

$$514 \quad C_{spy} = C_{o0} - C_{oeh} \quad (11)$$

515 where  $C_{i0}$  and  $C_{o0}$  are the initial and operation costs of the heating system, respectively,  $C_{ieh}$   
516 and  $C_{oeh}$  are the initial and operation costs of the electric water heater.

517 The efficiencies of the electric water heater and gas boiler are taken from [24] to be 0.95  
518 and 0.85, respectively. The electric water heater and gas boiler have a TES tank of 300 L. For  
519 the SHW systems, the sizes of the solar collector and outdoor TES tank are taken to be the  
520 same as those of the dual-source IX-SAASHP and therefore both systems have the same  
521 amount of solar thermal energy collected i.e. ca. 4.71 MWh. The heat provisions of the **three**  
522 heating systems for SH and HW over the year is ca. 11.19 MWh. It is noted that, for the serial  
523 system, the heat provision of ca. 10.82 MWh is insufficient to meet the requirement of thermal  
524 comfort sometimes and the rest heat needed is assumed to be provided by the auxiliary electric  
525 heaters with an efficiency of 0.95 for the purpose of economic analysis of the heating systems.

526 The current energy prices are taken from E.On Energy (a UK energy supplier) to be  
527 £212.17 per MWh for electricity and £ 41.18 per MWh for gas (prices in April 2021) [25].  
528 According to the “balanced pathway” scenario for net zero emission of greenhouse gases by  
529 2050 in the UK, the electricity generation costs via nuclear and gas with carbon capture and  
530 storage will be £85 and £80 per MWh and the sales of gas boilers will be phased out by 2033  
531 [2]. Wind and solar will provide 80% of electricity generation with a cost of £43 per MWh by  
532 2035. Therefore, the electricity price is expected to be £51.4 per MWh by 2035. The prices of

533 the components of the heating systems are obtained from an online market where the flat plate  
534 solar collector price is around £30 per m<sup>2</sup>, water tank price is £290 per 100 L, and a pump with  
535 a head of 15 m and a capacity of 15 L/min is around £10 [26]. All the three heating systems  
536 have a capacity of 8 kW. The systems are estimated to be easy to connect to current space  
537 heating and water heater. The installation costs are assumed to be 3 hours for SHW system and  
538 6 hours for SAASHPs with a cost of 80 per hour [27].

539 The results of economic analysis for 2021 and 2035 are listed in tables 8 and 9. As the  
540 electricity price will decrease by 75% by 2035, the payback period will be 4 times as that today.  
541 Though the gas boiler is the cheapest one today, they are expected to be phased out by 2033.  
542 The gas boiler boosted SHW is the second cheapest one and has a similar payback period to  
543 the parallel IX-SAASHP. This suggests that the parallel IX-SAASHP can be a good alternative  
544 for replacing gas boiler boosted SHW from now on. The payback period of the electric heater  
545 boosted SHW is almost 1.5 times as that of the parallel IX-SAASHP. The serial IX-SAASHP  
546 has the longest payback period due to its high initial cost. In general, IX-SAASHPs can save  
547 more operation cost than electric water heater and electric heater boosted SHW. Furthermore,  
548 since the initial cost can be partly covered by the UK Green Homes Grant [28], the parallel and  
549 dual-source IX-SAASHPs are of high potential value of applications in the UK.

550 Table 8: Results of economic analysis for electric heater, SHW and IX-SAASHP heating systems (2021)

	<b>Electric water heater</b>	<b>Gas boiler</b>	<b>Electric heater boosted SHW</b>	<b>Gas boiler boosted SHW</b>	<b>Serial IX-SAASHP</b>	<b>Dual-source IX-SAASHP</b>	<b>Parallel IX-SAASHP</b>	
Heat provision per year, MWh	11.19	11.19	11.19	11.19	10.82 + 0.37	11.19	11.19	
Efficiency/performance	0.95	0.85	0.95	0.85	SPF=5.5, 0.95	SPF=4.4	SPF=4.5	
Energy consumption per year, MWh	11.8	13.2	7.2	8.0	2.1	2.2	2.2	
Initial cost, £	collector	0	0	540	540	1350	540	540
	tanks	870	870	2320	2320	9570	2320	2320
	Heater/HP	60	15	60	15	460+60	1085	330
	pumps	0	0	20	20	30	30	30
	Installation	0	0	240	240	480	480	480
total	930	885	3020	2975	11630	4135	3380	
Operation cost, £	2499.1	542.1	1447.2	313.9	443.1	475.9	463.9	
Cost saving per year, £	-	1957.0	1051.92	2185.2	2056.1	2023.2	2035.2	
Payback period, year	-	-	2.1	1.0	5.4	1.7	1.4	

551

552 Table 9: Results of economic analysis for electric heater, SHW and IX-SAASHP heating systems (2035)

	<b>Electric water heater</b>	<b>Electric heater boosted SHW</b>	<b>Serial IX-SAASHP</b>	<b>Dual-source IX-SAASHP</b>	<b>Parallel IX-SAASHP</b>	
Heat provision per year, MWh	11.19	11.19	10.82 + 0.37	11.19	11.49	
Efficiency/performance	0.95	0.95	SPF=5.5, 0.95	SPF=4.4	SPF=4.5	
Energy consumption per year, MWh	11.8	7.2	2.1	2.2	2.2	
Initial cost, £	collector	0	540	1350	540	540
	tanks	870	2320	9570	2320	2320
	Heater/HP	60	60	460+60	1085	330
	pumps	0	20	30	30	30

Installation	0	240	480	480	480
total	930	3180	11950	4455	3700
Operation cost, £	606.0	367.9	107.2	115.4	112.5
Cost saving per year, £	-	254.8	498.1	490.1	493.0
Payback period, year	-	8.8	22.1	7.2	5.6

553

## 554 **7. Conclusions**

555 In this work, TRNSYS has been used to simulate the operation performances of serial,  
556 parallel and dual-source IX-SAASHPs for SH and HW in London. The economic analysis has  
557 also been conducted to forecast the market of the IX-SAASHPs under the energy scheme  
558 predicted for net-zero carbon emission by 2050 in the UK. The following conclusions can be  
559 drawn:

- 560 1. All the three IX-SAASHPs can achieve a yearly  $SPF_{sys}$  higher than 4.4, suggesting their  
561 potential to be applied for domestic heating under weather conditions in high latitude  
562 regions.
- 563 2. The **heat** provision of the serial IX-SAASHP is limited by the availability of solar irradiance.  
564 Since the solar energy is the sole heat source of the serial system, it requires large sizes of  
565 the solar collector and TES tanks, resulting in high installation cost and longer payback  
566 period.
- 567 3. The parallel IX-SAASHP has the simplest pipe connection and control function. It shows  
568 the highest  $SPF_{sys}$  and the most stable operation performance.
- 569 4. The dual-source IX-SAASHP shows much lower cost than the serial system and similar  
570 operation performance to the parallel system.
- 571 5. The parallel IX-SAASHP has the lowest payback period of 5.3 year and the dual-source  
572 IX-SAASHP has a payback period of 6.9 years.

573

## 574 **Acknowledgements**

575 The authors gratefully acknowledge the financial supports from the Joint PhD Studentship  
576 of China Scholarship Council (CSC) and Queen Mary University of London.

577

## 578 **Nomenclature**

579	$C_i$	initial cost difference
580	$C_{i0}$	initial cost of the studied system
581	$C_{ieh}$	initial cost of the electrical water heater
582	$C_{o0}$	operation cost of the studied system
583	$C_{oeh}$	operation cost of the electrical water heater.
584	$COP$	coefficient of performance
585	$C_{spy}$	cost saving per year
586	$HC$	heating capacity

587	$P_{pb}$	payback period
588	$Q_{ASHP, con}$	thermal energy obtained at the condenser of air source heat pump
589	$Q_{ce}$	clean energy used in the system
590	$Q_{HP, con}$	thermal energy obtained at the condenser of a heat pump
591	$Q_{HW}$	thermal energy for hot water
592	$Q_{SH}$	thermal energy for space heating
593	$Q_{su}$	solar energy used
594	$Q_{sup}$	thermal energy supply
595	$Q_{TES}$	thermal energy storage
596	$SF$	solar fraction
597	$SPF_{HP}$	seasonal performance factor of the heat pump
598	$SPF_{sys}$	seasonal performance factor of the system
599	$T_{amb}$	ambient air temperature
600	$T_{room}$	room air temperature
601	$T_{HWS}$	outlet temperature of hot water tank
602	$W_{ASHP}$	electricity consumed by the air source heat pump
603	$W_{HP}$	electricity consumed by a heat pump
604	$W_{pump}$	electricity consumed by all the pumps
605	$W_{SWHP}$	electricity consumed by the solar water heat pump
606	$W_{tot}$	total electricity consumed
607		
608	<b>Greek Letter</b>	
609	$\eta$	efficiency of electric heater and gas boiler systems
610		
611	<b>Abbreviation</b>	
612	ASHP	air source heat pump
613	DX-SAASHP	direct expansion solar-assisted air source heat pump
614	HP	heat pump
615	HW	hot water
616	HWS	hot water storage
617	IX-SAASHP	indirect expansion solar-assisted air source heat pump
618	PCM	phase change material



619	SAASHP	solar-assisted air source heat pump
620	SC	space cooling
621	SFH	single family house
622	SH	space heating
623	SHW	solar hot water
624	SWHP	heat pump used hot water from solar collector as heat source
625	TES	thermal energy storage
626	TRNSYS	TRaNsient SYstem Simulation program

627

## 628 **References**

- 629 [1] Department for Business, Energy & Industrial Strategy, Energy consumption in the UK, 2018
- 630 [2] Committee on Climate Change, The Sixth Carbon Budget -- The UK's path to Net Zero, 2020,  
631 <https://www.theccc.org.uk/publication/sixth-carbon-budget/>
- 632 [3] Long JB, Xia KM, Zhong HH, Lu HL, A YG, Study on energy-saving operation of a combined  
633 heating system of solar hot water and air source heat pump, *Energy Convers Manage* 2021; 220:  
634 113624.
- 635 [4] Kim T, Choi BI, Han YS, Do KH, A comparative investigation of solar-assisted heat pumps with  
636 solar thermal collectors for a hot water supply system, *Energy Convers Manage* 2018; 172: 472-  
637 484.
- 638 [5] Dongellini M, Naldi C, Morini GL, Influence of sizing strategy and control rules on the energy  
639 saving potential of heat pump hybrid systems in a residential building, *Energy Convers Manage*  
640 2021; 235: 114022.
- 641 [6] Chargui R, Awani S, Determining of the optimal design of a closed loop solar dual source heat  
642 pump system coupled with a residential building application, *Energy Convers Manage* 2017; 147:  
643 40-54.
- 644 [7] Yang LW, Xu RJ, Hua N, Xia Y, Zhou WB, Yang T, Belyayev Ye, Wang HS, Review of the  
645 advances in solar-assisted air source heat pumps for the domestic sector, *Energy Convers Manage*  
646 2021; 247: 114710.
- 647 [8] Freeman TL, Mitchell JW, Audit TE, Performance of combined solar-heat pump systems, *Solar*  
648 *Energy* 1979; 22: 125-135.
- 649 [9] Fraga C, Mermoud F, Hollmuller P, Pampaloni E, Lachal B, Large solar driven heat pump system  
650 for a multifamily building: Long term in-situ monitoring, *Solar Energy* 2015; 114: 427–439.
- 651 [10] Ji J, Cai JY, Huang WZ, Feng Y, Experimental study on the performance of solar-assisted multi-  
652 functional heat pump based on enthalpy difference lab with solar simulator, *Renew Energy* 2015;  
653 75: 381-388.

- 654 [11] Cai JY, Ji J, Wang YY, Huang WZ, Numerical simulation and experimental validation of indirect  
655 expansion solar-assisted multi-functional heat pump, *Renew Energy* 2016; 93: 280-290.
- 656 [12] Poppi S, Bales C, Heinz A, Hengel F, Chèze D, Mojic I, Cialani C, Analysis of system  
657 improvements in solar thermal and air source heat pump combisystems, *Appl Energy* 2016; 173:  
658 606–623.
- 659 [13] Liu Y, Ma J, Zhou GH, Zhang C, Wan WL, Performance of a solar air composite heat source  
660 heat pump system, *Renew Energy* 2016; 87: 1053-1058.
- 661 [14] Ran SY, Li XT, Xu W, Wang BL, A solar-air hybrid source heat pump for space heating and  
662 domestic hot water, *Solar Energy* 2020; 199: 347-359.
- 663 [15] Kutlu C, Zhang YN, Elmer T, Su YH, Riffat S. A simulation study on performance improvement  
664 of solar assisted heat pump hot water system by novel controllable crystallization of supercooled  
665 PCMs. *Renew Energy* 2020; 152: 601-612.
- 666 [16] Yerdesh Y, Abdulina Z, Aliuly A, Belyayev Y, Mohanraj M, Kaltayev A. Numerical simulation  
667 on solar collector and cascade heat pump combi water heating systems in Kazakhstan climates.  
668 *Renew Energy* 2020; 145: 1222-1234.
- 669 [17] Treichel C, Cruickshank CA. Analysis of a coupled air-based solar collector and heat pump water  
670 heater in Canada and the United States. IEA SHC Int Conf on Solar Heating and Cooling for  
671 Buildings and Industry 2019.
- 672 [18] Treichel C, Cruickshank CA. Energy analysis of heat pump water heaters coupled with air-based  
673 solar thermal collectors in Canada and the United States. *Energy* 2021; 221: 119801.
- 674 [19] Treichel C, Cruickshank CA. Greenhouse gas emissions analysis of heat pump water heaters  
675 coupled with air-based solar thermal collectors in Canada and the United States. *Energy*  
676 *Buildings* 2021; 231: 110594.
- 677 [20] Ma JL, Fung AS, Brands M, Juan N, Moyeed OMA. Performance analysis of indirect-expansion  
678 solar assisted heat pump using CO<sub>2</sub> as refrigerant for space heating in cold climate. *Solar Energy*  
679 2020; 208: 195-205.
- 680 [21] Dott R, Haller MY, Ruschenburg J, Ochs F, Bony J, The Reference Framework for System  
681 Simulations of the IEA SHC Task 44 / HPP Annex 38—Part B: Buildings and Space Heat Load,  
682 A technical report of subtask C—Report C1 Part B, International Energy Agency, 2013.
- 683 [22] World Health Organization, LEGIONELLA and the prevention of legionellosis, 2007.
- 684 [23] Chartered Institute of Plumbing and Heating Engineering,  
685 <https://www.ciphe.org.uk/consumer/safe-water-campaign/hot-water-scalds/>, [accessed on April  
686 22nd, 2021].
- 687 [24] Li H, Yang HX, Potential application of solar thermal systems for hot water production in Hong  
688 Kong, *Appl Energy* 2009; 86: 175–180.
- 689 [25] E.ON Energy, [https://www.eonenergy.com/for-your-home/products-and-services/best-deal-for-](https://www.eonenergy.com/for-your-home/products-and-services/best-deal-for-you/quote)  
690 [you/quote](https://www.eonenergy.com/for-your-home/products-and-services/best-deal-for-you/quote), [accessed on April 9th, 2021].

691 [26] <https://www.made-in-china.com>, [accessed on April 2nd, 2021].  
692 [27] Plumber Costs: 2021 Call Out Charges & Hourly Prices UK,  
693 <https://tradesmencosts.co.uk/plumbers/>, [accessed on October 11th, 2021].  
694 [28] Green Homes Grant: make energy improvements to your home,  
695 <https://www.gov.uk/guidance/apply-for-the-green-homes-grant-scheme>, [accessed on  
696 October 11th, 2021].  
697